IN VITRO COPPER NANOPARTICLE EXPOSURE INCREASES SUSCEPTIBILITY OF HUMAN LUNG CELLS TO INFECTION BY *STREPTOCOCCUS PNEUMONIAE*

by

Adam J. Aitchison

Submitted in partial fulfilment of the requirements
for the degree of Master of Science

at

Dalhousie University
Halifax, Nova Scotia
June 2018

DEDICATION PAGE

Many thanks to the unwavering support from my parents, and my sister. Thank you.

TABLE OF CONTENTS

LIST OF FIGURES

ABSTRACT

Streptococcus pneumoniae infection can cause pneumonia and invasive pneumococcal disease and is associated with significant morbidity and death worldwide. Moreover, welders are at increased risk of developing pneumococcal infections; which is thought to be a result of chronic overexposure to metal nanoparticles (NPs) found in welding fumes. To understand how NPs increase susceptibility to pneumococcal infection, we examined NP effects on cell viability, oxidative stress, and inflammation and whether changes in these outcomes sensitize lung cells to adhesion by different serotypes of *S. pneumoniae*. Using human lung A549 cells we showed that necrosis was the preferred mode of cell death after CuONP exposure, likely a result of the rapid dissolution of CuONPs into toxic copper ions. Moreover, CuONP exposure led to increased production of pro-inflammatory cytokines and increased production of reactive oxygen species to promote A549 cell death. In addition, pneumococcal adhesion was increased in A549 cells after CuONP exposure. However, pre-incubation with the antioxidant N-acetylcysteine prior to CuONP exposure led to decreased cell death as well as diminished pneumococcal adhesion. The autophagy inhibitor wortmannin was also shown to slightly ameliorate the cell death observed after CuONP exposure, however its effect on pneumococcal adhesion remains unknown. Taken together, these results show a possible relationship between oxidative stress, inflammation, cell death, and bacterial adhesion after CuONP exposure. This information is important because understanding the underlying biological mechanisms allows us to better provide the best methods and treatments to prevent or reduce the risks of NP- induced or -exacerbated pneumonia.

LIST OF ABBREVIATIONS USED

ALI	Air liquid interface
ALF	Artificial lysosomal fluid
COPD	Chronic obstructive pulmonary disease
CuONP	Copper oxide nanoparticle
CPC	Condensation particle counter
FACS	Flow-assisted cell sorting
FBS	Fetal bovine serum
HBSS	Hank's buffered saline solution
ICP-MS	Inductively coupled plasma-mass spectrometry
IF	Immunofluorescence
LPM	Litres per minute
LPS	Lipopolysaccharide
MOI	Multiplicity of infection
NAC	N-acetyl-cysteine
NIVES	Nanoparticle *in vitro* exposure system
NP	Nanoparticle
OD	Optical density
PAF	Platelet-activating factor
PAFR	Platelet-activating factor receptor
PBS	Phosphate buffered saline
PCV	Pneumococcal conjugate vaccine
PM	Plasma membrane
ROS	Reactive oxygen species
SEM	Scanning electron microscopy

SEM	Standard error of the mean
SMPS	Scanning mobility particle sizer
S.p	*Streptococcus pneumoniae*
TEM	Transmission electron microscopy
THB	Todd Hewitt broth + 0.5% yeast extract
TSA	Trypticase soy agar
URT	Upper respiratory tract
XRD	X-ray powder diffraction
XPS	X-ray photoelectron spectroscopy

ACKNOWLEDGEMENTS

This work could not be possible without the help and assistance of several groups. Specifically, I would first like to thank my supervisory members, Drs. Jason LeBlanc and Zhenyu Cheng for their excellent comments, suggestions and criticisms towards my project. Additionally, I would like to thank all the members of the HERC lab past and present for their insightful comments and help towards completion of my project. I thank you for your untiring support and enthusiasm.

This work was supported and funded by a student grant from the Canadian Institute for Health Research (CIHR), and an operating grant from the Nova Scotia Lung Association.

Finally, I would like to thank Dr. Jong Sung Kim for consistently raising the bar and pushing me to do my very best. I truly appreciate the patience, input and criticisms, which allowed me to further develop a true appreciation for scientific research.

CHAPTER 1: INTRODUCTION

1.1 Streptococcus pneumoniae

1.1.1 Infection by Streptococcus pneumoniae

Pneumonia remains one of the most common causes of death in industrialized countries with an associated mortality rate of up to 30% **[1]**. Many pneumonia cases are caused by infection with *Streptococcus pneumoniae (S. pneumoniae). S. pneumoniae* normally colonizes the mucosal surfaces of the airways asymptomatically **[2]**. However, *S. pneumoniae* can migrate into sterile parts of the airway, and into systemic circulation, resulting in disease development and progression **[3]**. The mechanisms underlying this 'switch' from colonization to the causing of disease are not well understood, but is thought to involve intimate interactions of *S. pneumoniae* with the epithelial cells of the lung, which is the first required step in infection **[3,4]**. Therefore, it has become increasingly important to fully understand host-pathogen interactions to prevent disease initiation and development.

1.1.2 Epidemiology of S. pneumoniae infections

Certain patient populations are more susceptible to infection by *S. pneumoniae,* such as immunocompromised individuals. In children, it has been estimated that 20% of all deaths under five years of age are attributed to pneumococcal infections **[5]**. The elderly are another at-risk group for developing, and subsequently dying from pneumonia **[6]**. However, pneumonia commonly presents in elderly patients with pre-existing co-morbidities such as ischemic heart disease, chronic obstructive pulmonary disease (COPD) or immunosuppression. **[7,8]**. Currently, the best approach for treating pneumococcal infections in children and elderly are with antibiotics, such as penicillin. Not surprisingly,

it was shown that administering antibiotics within 8 hours of hospitalization in the elderly improved survival significantly [6]**.** Additionally, it has been suggested that over 5% of all childhood deaths from pneumonia could be prevented if there was better coverage and utilization of antibiotics worldwide **[9]**. As a result, extensive treatment with antibiotics may limit the burden that *S. pneumoniae* has on the population.

Empiric therapy for suspected cases of *S. pneumoniae* include the penicillin class antibiotics (e.g. β-lactams) and macrolides (e.g. azithromycin) **[10]**. However, antibiotic resistance to these first-line antibiotics has been increasing, making treatment more difficult **[11]**. Currently, fluoroquinolones remain an effective treatment for those at risk, or that have been diagnosed with *S. pneumoniae* resistant to first-line antibiotics. However, it is possible that fluoroquinolone-resistance could develop. So far, this has not been widespread in Canada **[12].** On the other hand, the development of new antibiotics has been slowing **[13]**. As a result, it has become increasingly important to identify certain groups that are at risk for developing pneumonia so that preventative interventions, such as targeted vaccination programs may be designed and implemented. Epidemiological evidence taken from 2000-2004 has shown that occupations entailing exposure to metal fumes, principally welders, are at increased risk of developing and dying from pneumonia **[14,15]**. However, the strength of this association is not completely understood.

1.1.3 S. pneumoniae virulence factors

S. pneumoniae expresses an array of virulence factors in coordination to facilitate adhesion and subsequent invasion **[16]**. These include antiphagocytic factors, such as biofilm matrices, or polysaccharide capsules **[17]**. Another factor, pneumolysin, is a pore-forming toxin, which is lytic to all cells with cholesterol present in their plasma membrane

(PM) **[18]**. *S. pneumoniae* also has the capability to sequester and take up iron through the secretion of siderophores and upregulation of iron transporters on their cell surface **[19]**.

Host recognition and binding are important for *S. pneumoniae* pathogenesis. There are many different host-pathogen receptor interactions, with well-characterized receptors such as platelet-activating factor receptor (PAFR) expressed on the surface of cells, such as type II alveolar cells **[20]**. Normally, PAFR binds to platelet-activating factor (PAF, 1-O-alkyl-2-acetyl-sn-glycero-3-phosphocholine), a potent phospholipid cell mediator, and this binding induces platelet aggregation **[21,22]**. However, *S. pneumoniae* also has PAF present in their cell wall, and as a result can bind to this receptor, facilitating its colonization **[23]**. Indeed, blocking of PAFR with an antagonist led to impaired pneumococcal invasion, resulting in improved survival of mice. These results suggest that PAFR is indispensable for virulence of *S. pneumoniae*. **[24]**.

1.1.4 The role of capsule and serotype in virulence and prevalence of disease

The capsule is perhaps the most important virulence determinant of *S. pneumoniae* and is what dictates its serotype **[25,26]**. The capsule prevents mucosal clearance and inhibits complement to help promote virulence **[27,28]**. As a result, *S. pneumoniae* that produces sufficient capsule is capable of invading surrounding areas to facilitate invasive pulmonary disease **[29]**. However, for colonization of the epithelial cells to occur, the capsule must undergo a type of phase-variation, which involves changes in the expression of genes required for adhesion (eg: adhesins) **[30-32]**. In simpler terms, an invasive *S. pneumoniae* serotype produces more capsule than an *S. pneumoniae* serotype that colonizes the epithelia. It is likely that this phase-variation switch contributes to the pathogenesis of *S. pneumoniae* in causing disease **[33]**.

Different capsular serotypes of *S. pneumoniae* provide varying risks of developing invasive pulmonary disease **[34]**. However, the most prevalent serotypes are not necessarily the most invasive **[35]**. On the other hand, serotypes that are more frequently found to colonize individuals are granted a higher chance to cause disease **[35].** As a result, vaccines are designed for the most prevalent cause of invasive pneumococcal disease (IPD) at that time **[36]**. Thus, it is imperative that surveillance of pneumococcal diseases be an ongoing process; as distribution of *S. pneumoniae* capsular serotypes will always be changing. For example, if you reduce the prevalence of one serotype, there may be another serotype that fills that niche **[37]**. This is referred to as serotype replacement.

In welders, there was increased prevalence of serotypes 4, and 8, among others, and all cases were caused by serotypes targeted by the 23-valent polysaccharide vaccine **[14]**. Specifically, the study was done between 2000-2004 to determine the incidence of pneumonia in welders compared to non-welders. Although the pneumococcal conjugate vaccine (PCV7) was introduced around this time in Alberta, it is only recommended for infants and children - not adults **[38]**. On the other hand, the pneumococcal polysaccharide vaccine (PPSV23) is recommended for the elderly and individuals at high risk for IPD. Currently, welders are not a group in Canada to be recommended to receive pneumococcal vaccines, despite growing evidence of increased risk of pneumonia and IPD.

1.1.5 The relationship between welding and pneumococcal disease

There is evidence linking welding occupations with increased risk of developing pneumococcal disease, going back as far as the 1940s **[39-41].** From these findings came policies, especially in the U.K, for welders to get vaccinated against pneumonia **[42]**. However, it is often difficult to derive conclusions from epidemiological evidence as there

may be confounding effects, such as smoking, which is a known risk factor for pneumococcal disease **[43]**. Nonetheless, when welding fumes were collected and incubated with human lung cell lines (A549), there was a significant increase in PAFR mRNA levels, suggesting a potential mechanism by which welding fumes increase adhesion of *S. pneumoniae* **[44]**. However, welding fumes are heterogeneous in composition, and include many different metals such as iron, copper, zinc, and aluminum, so it may be difficult to determine the role of individual metals in causing disease **[45]**. Most particles generated during welding are nanosized (less than 100 nm in diameter) and are likely responsible for the increased susceptibility to *S. pneumoniae* infections **[46-49]**. However, the effects of nanosized particles on pneumococcal adhesion are not well known.

1.2 Nanoparticles, inflammation, and cell death responses

1.2.1 Nanoparticles: Friend or foe?

Nanotechnology is at the forefront of scientific discovery and innovation and allows us to explore and create new materials, called nanoparticles (NPs) which are defined as having a diameter less than 100 nm **[50]**. NPs are used extensively in our everyday lives and can be found in many things, such as electronics, foods, cosmetics, and medicine **[51-53]**. For example, titanium dioxide NPs are a large component of sunscreens, due to their ability to reflect ultraviolet light **[54]**. As scientific innovation and nanotechnology continue to flourish and progress, the usage and development of NPs will continue to rise with it.

However, as with most new technology, the risks to public health and the environment remain poorly understood. The ability of policies and regulations to keep up with rapid scientific discovery and innovation has been difficult due to a general lack of

data on NP-toxicity. Interestingly, the US Food and Drug Administration (FDA) has issued guidance documents related to the use of NPs in certain regulated products, such as cosmetics and foods as recently as 2014 **[55]**. The FDA acknowledges that the safety of NPs is not well known or understood, and recommends that any FDA-regulated product made with, or that may contain NPs be evaluated for safety on a product to product basis. This is a step in the right direction, in the hope that we may limit the exposure to NPs that arise from engineered design. However, NPs can arise through non-engineered means, such as combustion of fossil fuels, and generation of welding fumes **[46]**. These NPs can be readily inhaled, and may result in unwanted toxic effects, such as the generation of ROS and inflammation.

1.2.2 Inflammation and oxidative stress

Inflammation is a complex biological response to a wide range of harmful stimuli and presents diagnostically as pain, heat, redness and swelling. Stimuli include harsh physical conditions, such as extreme heat (burns) or extreme cold (frostbite) **[56,57]**. Moreover, inflammation can be induced by biological agents, such as bacteria or viruses **[58],** or chemical irritants and toxins **[59]**. Despite the wide range of causes, the function of inflammation is unified. First, inflammation eliminates the cause of injury to remove damaged cells or tissues that were killed in the exposure **[60]**. This effectively prevents the spread of damage. Second, the inflammatory response can promote adaptive healing to initiate tissue repair **[61]**. It is important to note, however, that too much inflammation is detrimental to the host organism, despite good intentions. Conditions, such as atherosclerosis, allergies or asthma result from aberrant inflammatory responses **[62-64]**.

Oxidative stress is a major inflammatory determinant triggered by oxidation of cellular components by oxidants **[65]**. These include the superoxide anion, which is formed during oxidative phosphorylation by the electron transport chain **[66]**. Additionally, hydrogen peroxide (H_2O_2) can be formed from superoxide and is readily released from cells by passive diffusion **[67,68]**. In terms of reactivity, the hydroxyl radical (•OH) is very reactive and attacks almost all cellular components **[69].** On the other hand, peroxide radicals have the propensity to oxidize lipid membranes to increase permeability and membrane disruption **[70]**. Taken together, oxidants and resultant ROS can damage lipid membranes, DNA, RNA, and proteins to collectively disrupt cellular homeostasis, leading to activation of cell repair mechanisms, or if the damage is to much, cell death.

Normally, intracellular oxidant levels are kept low through cellular antioxidant capacity or repair mechanisms. For example, thymine glycols produced by DNA ionization can be removed through base excision repair **[71]**. There exists specific enzymes with antioxidant functions, such as superoxide dismutase, catalase, and glutathione peroxidase **[72,73]**. Antioxidant molecules such as thiols or ascorbic acid can also balance the oxidative load **[74,75]**. However, antioxidant capacity can be exceeded through saturation of enzymes and depletion of antioxidant molecules if a certain stressor is capable of generating a large burst of oxidants **[76]**. If oxidants are not neutralized in a timely manner, they activate proinflammatory pathways such as NF-kB, TNF-alpha and Nrf-2 **[77-79]**. It has been shown that the Nrf-2 pathway leads to upregulation of antioxidant enzymes to alleviate the oxidative stress response **[80,81]**. Moreover, upregulation of transcription factors such as NF-kB result in production of cytokines and chemokines involved in inflammation **[82]**. However, production of cytokines, such as interleukins can be a double-

edged sword **[83,84]**. If the stressor is acute but minute enough, then the cell copes with the toxicant through transient oxidative stress, and upregulation of proinflammatory pathways to restore homeostasis. However, chronic exposure leads to chronic oxidative stress and chronic inflammatory states. A hallmark example is that of Alzheimer's where peroxidised lipids and proteins accumulate in brain cells, leading to chronic inflammation **[85]**. Moreover, chronic inflammation is also seen in aging, where the normal antioxidant capacity is diminished, oxidants accumulate, resulting in inflammation **[86]**.

1.2.3 Metals promote oxidative stress and inflammation

It is important to identify oxidant sources so that future exposures can be limited or prevented. Not surprisingly, metals have been shown to induce oxidative stress and promote inflammation **[87,88]**. However, complete avoidance to metals is not possible since some metals are essential micronutrients. For example, iron and copper are found in cytochromes required for oxidative phosphorylation **[89]**. Additionally, copper and manganese are found in superoxide dismutases responsible for limiting oxidative stress **[90]**. Iron has an important role in redox chemistry as it undergoes a process known as the Fenton reaction **[91]**. Fe^{2+} is oxidized by H_2O_2 to form Fe^{3+}, •OH and a hydroxide ion. Additionally, copper also participates in a similar Fenton reaction **[92]**. All free radicals that are produced by Fenton reactions react with biological compartments to induce oxidative stress and cause inflammation. As a result, abnormally high levels of iron and copper are detrimental to the cell. Normally iron and copper are kept sequestered by ferritin or ceruloplasmin, respectively, so free ion levels are kept to a minimum **[93,94]**. However, abnormal sequestration leads to toxicity and disease. For example, Wilson's Disease is caused by the inability to link Cu to ceruloplasmin, which prevents excretion of copper,

promotes oxidative stress, which leads to hepatitis, fibrosis, and cirrhosis **[95]**. If left untreated, Wilson's Disease is fatal, but can be managed throughout a diet low in copper or with copper chelators **[96]**. However, since copper is required for superoxide dismutase, avoidance of copper will also lead to oxidative stress.

1.2.4 Metal NPs as a cause of oxidative damage

Metal NPs are a source of metal ions to promote oxidative stress and inflammation. Indeed, many studies have shown metal NPs to be toxic. For example, ZnO and cadmium sulfide NPs promoted oxidative stress and formation of ROS through activation of the NFkB pathway **[97,98]**. Moreover, AgNPs have been shown to induce mutations and promote oxidative stress in mouse lymphoma cells **[99]**. Researching the toxic potential of metal NPs is difficult. Size, dissolution rate into toxic ions, and solubility can all affect the toxicokinetics and change the mechanism of action. For example, NiNP exposure was shown to be toxic to zebrafish, whereas which Ni ions were not, suggesting a role for compartmentalization of NPs **[100]**. Indeed, AgNPs were shown to require uptake by endocytosis and subsequent dissolution by low lysosomal pH for full toxic potential **[101]**. Moreover, coating of various NPs with different caps, such as citrate have been shown to change toxicity **[102]**. In the case of some CuNPs, a low pH has been shown to facilitate dissolution into toxic ions **[103]**. All of these NP characteristics must be taken into account when assigning a toxic profile and as a result, metal NPs can prove troublesome for toxicity studies.

1.2.5 Apoptosis

Apoptosis, also known as programmed cell death (PCD), is characterized by specific targeting and dismantling of key cellular compartments, resulting in finely-

controlled cessation of metabolic processes within the cell **[104]**. These processes are largely accomplished by a family of proteases, called caspases, which recognize specific targets with specific amino acid motifs to cause proteolysis **[104]**. Caspases can be largely classified as either being initiator or effector caspases. The initiator caspases, which include caspase 8, contain specific death effector domains (DED) which interact with upstream effectors **[105]**. For example, caspase 8 interacts with Fas-activating death domains during TNF-alpha binding. Upon activation, initiator caspases interact with downstream effectors to promote apoptosis **[105]**. For example, caspase 9 interacts with APAF-1 to form the apoptosome **[106]**. These initiation processes activate effector caspases. As the name suggests, effector caspases, such as caspase 3 effectively carry out the cleaving of cellular targets, governed by specific recognition sites.

Apoptosis can be either extrinsic or intrinsic. The extrinsic pathway is activated by external stimuli by engagement of death receptors on the cell surface. For example, Fas ligand on cytotoxic T lymphocytes can bind to FasR on target cells **[107]**. This results in the formation of a death-inducing signaling complex (DISC), which activates caspase 8 and subsequent effector caspase activation **[107]**. On the other hand, intrinsic apoptosis is initiated in response to internal stimuli, such as DNA damage. This ultimately leads to mitochondrial permeabilization, leading to activation of effector caspases **[108]**. It is important to note that apoptosis is tightly controlled as to not disrupt normal cellular function **[109]**. Additionally, apoptosis prevents disruption to neighboring cells and the surrounding architecture **[110]**. As a result, inflammatory responses are not induced. The cell breaks into apoptotic bodies, and cells exposing phosphatidylserine on the outer leaflet of the PM signal to phagocytes to engulf the cell, destroying it **[111]**.

1.2.6 Necrosis

As opposed to apoptosis, necrosis is largely considered to be uncontrolled and unregulated, and is met with considerable levels of inflammation. Necrosis is often initiated when ATP is thoroughly depleted, which leads to deactivation of ATPases required for ion transport **[112]**. This leads to increased water influx into the cell and considerable cellular swelling. Concurrently, there is rapid destruction of cellular compartments by non-apoptotic mechanisms leading to a much more rapid demise [113]. Whereas apoptotic cells can display recognition signals for phagocytes, necrotic cells proceed with uncontrolled cellular lysis, leading to a release of cellular contents before the cell can be recognized and engulfed by phagocytes **[114]**. These released cellular molecules act as signals to promote inflammatory processes, and to recruit various immunomodulatory cells such as neutrophils. It is important to note, however, that the delineation between necrosis and apoptosis is not entirely clear. Some groups have suggested that necrosis can occur through regulated mechanisms involving receptor interacting protein kinase (RIPK), referred to as necroptosis **[115]**. Nonetheless, many studies only consider two outcomes: apoptosis or necrosis when describing cell death.

Toxicology testing must consider multiple modes of cell death when assigning a toxicological profile to a compound. For example, agents that induce low amplitude responses are associated with apoptosis, whereas a higher amplitude response would be associated with necrosis **[116]**. This amplitude response is largely dictated by toxicant dose where small doses favor apoptosis, and larger doses favor necrosis. Indeed, 5 Gy of ionization promoted apoptosis in MG-63 osteosarcoma cells, whereas 30 Gy promoted necrosis **[117]**. It is important to note that intermediary doses do not result in a mixed-

mode of apoptosis. In other words, a cell can only die by one mechanism **[118]**. However, a population of cells may be exposed to different doses of a toxicant (e.g. proximity), resulting in a population of cells that experience cell death by different mechanisms.

It can be difficult to predict the preferred mode of cell death after toxicant exposure. Some studies suggest that the number of mitochondria damaged during the insult determines the ultimate fate. Indeed, it has been shown that injury that causes little mitochondrial dysfunction promotes apoptosis, whereas an injury that causes a lot of mitochondrial dysfunction promotes necrosis **[119]**. Elucidating the biological mechanisms of injury and mode of cell death after exposure to a toxicant provides data for future research and to provide evidence for public health agencies to enact policies to limit exposure.

1.2.7 Metal NPs and cell death

Metal NPs have been shown to induce inflammation and oxidative stress and promote cell death. Metal NPs can promote apoptosis or necrosis and the response is primarily determined by dose. For example, ferric oxide and ferriferous oxide NPs have been shown to promote apoptosis in human umbilical endothelial cells and increase the risk for atherosclerosis **[120]**. NiNPs have been shown to induce apoptosis in A549 cells and this was mediated through inhibition of p53 **[121]**. Additionally, AgNPs were shown to promote cell cycle arrest, and inhibit intracellular glutathione production to promote apoptosis **[122,123]**. Although apoptosis appears to be the major pathway of NP-induced cell death, there have been some studies showing a necrotic response. For example, zinc oxide NPs induced necrosis at high concentrations, however promoted apoptosis at lower

concentrations. Another study showed that metal NPs composed of Ti, Al, and Cr also promoted necrosis as concentration increased **[124]**.

Most toxicants experience a strong dose-response relationship but metal NPs have other determinants that complicate this relationship. As mentioned previously, a key determinant is the dissolution rate, which determines the amount of toxic ions to which a cell can be exposed **[125].** If there is no dissolution, then toxicity would not be predicted to readily occur. For example, zinc oxide NPs undergo rapid dissolution (within hours), and this acute response may explain why necrosis occurred at sufficient doses **[98].** Copper NPs exhibited similar dissolution kinetics as zinc, and were also shown to be acutely toxic **[126]**. Indeed, surgical gowns have been impregnated with copper NPs due to their fast dissolution into toxic Cu^{2+}, acting as an effective bactericidal agent **[127]**. Interestingly, CuONPs have been shown to be more toxic to mammalian cells than an equivalent dose of Cu^{2+} ions, suggesting that other mechanisms contribute to toxicity **[128]**. To further complicate metal NP toxicity, metal NPs can have different surface charges depending on their environment, leading to differences in aggregation, which can affect NP dissolution and reactivity **[129].** Indeed, CuONP toxicity depends on pH and presence of proteins, amino acids, and other components **[130]**.

As a result, toxicological studies that utilize a particular metal NP may provide a different toxicological profile and cell death mechanism than a similar study that uses the same type of metal NP, but with slightly different condition parameters. Taken together, it is important to not use only one study to provide evidence of metal NP toxicity. Rather, it is the summation of all toxicological data that helps us make informed decisions.

1.2.8 Inhalation of NPs is a major exposure route

The respiratory tract can be largely divided into two major areas: the upper and lower respiratory tracts, separated by the pharynx **[131]**. As part of the upper respiratory tract (URT), the proximal airways and nasal passages are composed of specialized cell types, such as ciliated and mucosal cells that comprise a mucosal layer **[132]**. This mucosal layer plays an important function in defense and immunity. When small agents, such as bacteria and viruses are inhaled, they are trapped in this mucosal layer and are removed by mucociliary clearance (eg: blowing the nose, or sputum) **[133]**. Additionally, many inhaled agents may illicit an immune response. Indeed, it was shown that nasal epithelia have certain pattern-recognition receptors that can recognize, and subsequently activate immune responses by interaction with antigens **[134]**. On the other hand, inhaled NPs may be too small to properly stimulate an immune response, and must rely on mucociliary clearance as the primary mechanism to remove NPs from the body **[135,136]**. Indeed, NPs of sufficient size can deposit on the nasal mucosa through impaction or diffusion and later cleared. Particle size is the single most important determinant in determining where a NP deposits **[137]**. Whereas a larger particle will be trapped in the nasal passages and be readily cleared, smaller particles can penetrate deep into the lung.

In respiratory toxicology, particles can be classified as either: dusts (> 1μm; generated from grinding), fumes (<0.1 μm; from metal or oil condensation), smoke (<0.5 μm carbon particles; from combustion), mists (2-50 μm water droplets; from spraying), fog (< 1 μm water droplets; made through water vapour condensation), or smog (>0.01-50 μm air pollution) **[137,138]**. Small ultrafine nucleation particles are created through nucleation of gas phase emissions. These particles can further condense as conditions cool

which further promotes interactions with gases, such as sulfates. Electrostatic interactions can promote further aggregation and agglomeration of these fine particles to form larger particles **(Fig 1.1)**. On the other hand, very coarse particles are generated through mechanical means, such as grinding. Larger particles do not readily remain suspended in the air as they relatively quickly settle as compared to their smaller counterparts **[138]**. The fact that smaller particles remain in the air for longer periods of time, and can more readily penetrate deep into the respiratory tract provides additional opportunity for exposure and toxicity.

Understanding the mechanisms of NP deposition in the respiratory tract can provide key insights into understanding the resultant toxic responses. Particles deposit by four main mechanisms, and this is a gradient where smaller particles penetrate more deeply **[137] (Fig 1.2)**. The first is impaction, where large particles (> 10 μm) collide with the airway linings as a result of fast airflow, and airway bifurcation. The second is interception (~1 μm), where the trajectory of a particle approaches an airway surface, leading to contact and subsequent deposition. The third is sedimentation, and occurs in the smaller bronchi (~0.5 μm). Due to extensive branching of the bronchioles, air-flow is decreased leading to decreased buoyancy of NPs. As a result these NPs succumb to gravity and deposit onto bronchiolar surfaces. The fourth is diffusion, and occurs to small particles (<0.5 μm) due to random motion imparted by gas (air) molecules **[137]**. Although diffusion can occur in the proximal/nasal airways, it also permits the deposition of very small particles into the alveolar regions of the lung.

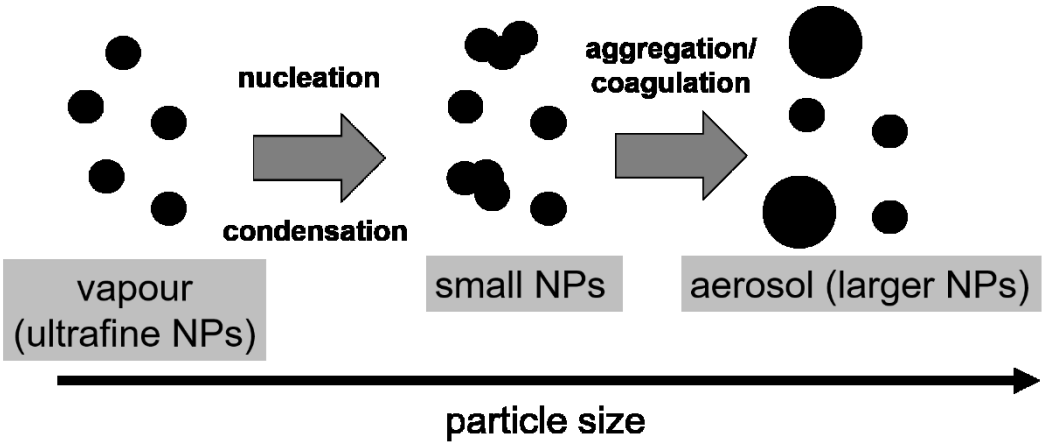

Figure 1.1. Stepwise formation of nanoparticles. Ultrafine particles nucleate and condense with vapors to form increasingly larger particles. These NPs can continue to increase in size, where they can aggregate and coagulate to form larger NPs. Particle size increases in the figure from left to right.

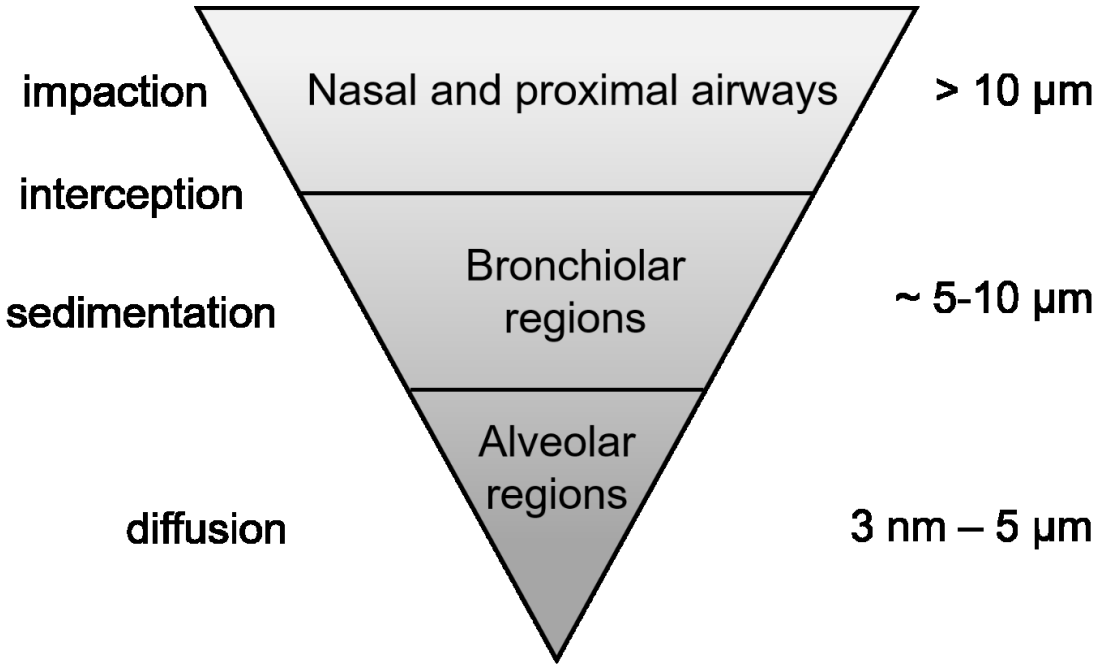

Figure 1.2. NP penetration and deposition in the lung. Larger particles are trapped in the nasal and proximal airways and are readily removed from the body. As NP size decreases, penetration increases, with intermediate particles trapped in the bronchiolar regions, and very small NPs deposited onto the alveolar regions.

Since the alveoli are where gas exchange occurs with the systemic circulation, exposure to small NPs can lead to many problems **[139]**. NPs may be too small to induce an immune response, too small to be recognized by resident macrophages, and possibly small enough to move through membranes into circulation **[135]**. As a result, inhaled NPs have been shown to promote lung injury. For example, carbon nanotubes (CNTs) have been shown to cause fibrosis, and asthma through pulmonary inflammation **[140]**. Another study showed that 14 nm carbon NPs intensively aggravated lipopolysaccharide (LPS)-induced lung inflammation showing that NPs can act synergistically to disease-mediated lung injury leading to worse outcomes **[141]**.

Welding fumes are enriched in metal NPs **[45]**. As a result, they are readily inhaled by welders and deposit onto lung cells. As a result, these metal NPs provide a metal source to promote oxidative stress, inflammation, and cellular injury/death.

1.3 Toxicity of inhaled NPs in welders?

The evolving paradigm is that 1) metal NPs are readily inhaled, and deposit onto the alveolar surfaces of lung cells and 2) metal NPs promote oxidative stress, inflammation, which culminates in cell death by either apoptosis or necrosis. As a result, occupations that entail high exposures to metal NPs may put the health of workers at risk.

As described previously, welders are at increased risk for pneumococcal infections, but the underlying biological mechanisms are not well known. It is likely that metal NP exposure leads to increased bacterial infection mediated through a combination of oxidative stress, inflammation, and cell death. To support this hypothesis, copper NP exposure impaired host defense against *Klebsiella pneumoniae* and induced a dose dependent decrease in bacterial clearance in mice, which resulted from increased oxidative

stress, and generation of free radicals that damaged the lung epithelium **[142]**. Although exposure to welding fumes *in vitro* led to increased adhesion, it is not known whether exposure to specific individual metal NPs, such as copper would elicit a similar effect **[44]**.

Overall, pulmonary toxicity and pathophysiology of NPs is an important issue that deserves our attention and is something we should investigate more fully.

1.4 Hypothesis and research questions

As previously mentioned, welders are 1) at increased risk of developing and dying from pneumonia, and 2) chronically exposed to fumes enriched in metal NPs such as iron, copper, and zinc. My central hypothesis is that inhalation of metal NPs commonly found in welding fumes, specifically copper, increases susceptibility of welders to pneumonia caused by *S. pneumoniae* through increased adhesion and/or cellular damage to human lung cells. A graphical representation of the hypothesis can be seen in **Figure 1.3**.

To test my hypothesis, I will address four research questions:

1) Are copper-based NPs toxic to human lung epithelial cells?

Although copper NPs have been previously shown to be toxic to lung cells *in vitro*, the cytotoxic potential still needs to be established. CuONPs will be synthesized *de novo*, and will be fully characterized to establish proper toxicological parameters. Since size, shape and dissolution kinetics can all influence the toxicological potential, all of these parameters will be measured and reported.

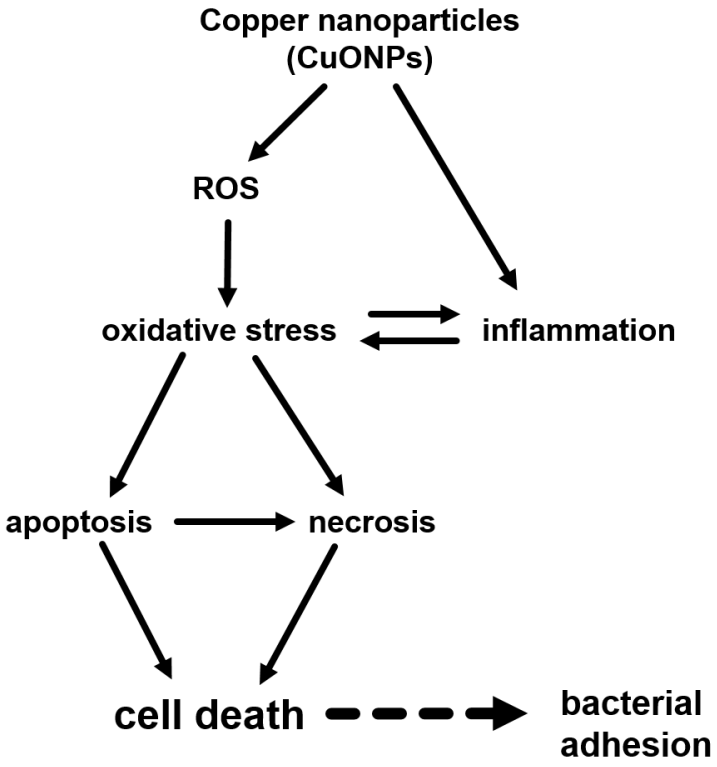

Figure 1.3. A proposed mechanism by which CuONPs are thought to increase *S. pneumoniae* adhesion. CuONPs promote oxidative stress and inflammation, which leads to cell death by either apoptosis or necrosis. This cell death response is thought to lead to bacterial adhesion. It is also possible that upstream processes such as inflammation can influence bacterial adhesion independent of cell death processes.

2) ***Is pneumococcal adhesion to human lung epithelial cells increased after exposure to copper-based NPs****?*

It has been previously shown that copper NP (CuONP) exposure resulted in enhanced bacterial infection and reduced clearance in mice. Since adhesion is a prerequisite step for infection, it is hypothesized that there will be increased adhesion of *S. pneumoniae* to lung cells after CuONP exposure. To address this, I will expose A549 human lung cells to CuONPs and then perform a bacterial adherence assay followed by quantitative bacterial cell culture to measure adhesion capability.

3) What is the mechanism underlying this enhanced adhesion after CuONP exposure?

As mentioned before, there is increased production of ROS after NP exposure. It is possible that increased ROS leads to increased adhesion as well as cytotoxicity. The importance of ROS will be determined by culturing cells with or without N-acetyl-cysteine (NAC) to limit ROS generation during NP-exposure, and bacterial adhesion and cytotoxicity will be measured. Additionally, apoptosis and necrosis are increased after CuONP exposure, and their importance will be determined with the use of apoptotic and necrotic inhibitors.

4) ***Does the mode of CuONP delivery affect pneumococcal adhesion?***

Although submerged cell culture systems remain a gold standard, they may not truly represent proper lung physiological conditions. As a result, CuONPs will be generated using a spark discharge system and delivered to human lung cells at an air-liquid interface. These particles will also be characterized with respect to size and shape, and their ability to increase *S. pneumoniae* adhesion will be measured.

CHAPTER 2: MATERIALS AND METHODS

2.1 Materials

RPMI 1640 media, phosphate buffered saline (PBS), fetal bovine serum (FBS), penicillin/streptomycin, gentamycin, trypsin-EDTA (0.25%), alamarBlue reagent, cyclosporine, wortmannin, and common lab reagents were purchased from Thermo-Fisher unless otherwise specified (Waltham, MA). C11-BODIPY$^{581/591}$, DCFDA, Annexin V-FITC Apoptosis Detection Kit, human IL-6/IL-8/MCP-1 magnetic bead kits, and 7-AAD were purchased from Invitrogen/Molecular Probes (Burlington, ON). Tryptic soy blood agar plates (TSA II) were purchased from BD Biosciences (Mississauga, ON). Copper(II) sulfate, iron(II) chloride, sodium hydroxide, and N-acetyl cysteine (NAC) were purchased from Sigma-Aldrich (St. Louis, MO). Z-VAD-fmk and necrostatin-1 was purchased from Enzo Life Sciences (Brockville, ON). Transwell culture inserts were purchased from Corning (Corning, NY). Lastly, all purified gases (N_2, CO_2, and O_2) were purchased from Praxair Canada (Dartmouth, NS).

2.2 CuONP exposure using a submerged culture system

2.2.1 Synthesis of NPs

Copper (II) sulfate (0.6 g) was dissolved in 25 mL of MilliQ water (150 mM). The solution was saturated with N_2 to purge dissolved O_2. The solution was heated to 70º C and NaOH (0.4 g) was slowly added (400 mM). The NP-formation reaction proceeded for 30 minutes with continuous stirring at 70 ºC. Afterwards, the solution was cooled to room temperature, subjected to centrifugation (13,000 G), and the supernatant discarded. MilliQ water was added and the NPs dispersed, followed by subjection to centrifugation (13,000

G), and discarding of the supernatant again. The NPs were washed with acetone to remove excess water, subjected to centrifugation, and the supernatant discarded. Finally, the NPs were incubated at 50 ºC overnight. The NPs were collected, and finely grounded using a mortar and pestle.

2.2.2 Size determination of NPs for submerged exposures

NPs were suspended in MilliQ water to 0.1 mg/mL and sonicated at 60 Hz for 5 minutes to ensure complete dispersion. The solution was aerosolized using a TSI 3076 constant output atomizer and water vapour was removed using a TSI 3062 Diffusion dryer to obtain dried NPs. The size distribution of the dried particles was analyzed using a size mobility particle sizer (SMPS; TSI 3085 or 3080) coupled to a condensation particle counter (TSI 3775).

2.2.3 Transmission electron microscopy (TEM)

NPs were suspended in absolute ethanol to 0.1 mg/mL and sonicated at 60 Hz for 5 minutes. The solution was added dropwise to Formvar-coated copper TEM grids and evaporated between each drop. Grids were analyzed with a FEI Technai-12 transmission electron microscope to determine the size and morphology of CuONPs.

2.2.4 X-Ray powder diffraction (XRD)

XRD was done in accordance to procedures outlined in Hatchard *et al.* **[143]**. Briefly, CuONPs were deposited onto an XRD well-plate, and data was collected using a JD2000 diffractometer equipped with a Cu target X-ray tube and a diffracted beam monochromator. The generator was set for 40 kV and 30 mA. Data was collected between $2\Theta = 20°$ and 75° at 0.02° intervals. The count time was 8 s per point, giving a total scan time of 7 h.

2.2.5 X-Ray photoelectron spectroscopy (XPS)

XPS was done in accordance to procedures outlined in Bayindir *et al.* **[144]**. Briefly, CuONPs were submitted to the Dalhousie Physics Department and analyzed using a Multilab 3000 XPS system. The data was collected with a dual anode X-ray source with MgKα irradiation.

2.2.6 Dissolution of NPs in submerged conditions

NPs were suspended in the appropriate solution to be tested for dissolution experiments. Suspensions (1 mL) were incubated at 37 ºC and supplemented with 5% CO_2 in a humidified atmosphere to mimic physiological conditions. At the appropriate times, solutions were collected, and subjected to centrifugation at 13,000 G to pellet any remaining NPs that had not dissoluted. To ensure complete removal of NPs, the solutions were passed through a 0.2 µM filter. Finally, samples were diluted accordingly with 2% nitric acid for inductively coupled plasma-mass spectrometry (ICP-MS) analysis.

For a complete dissolution positive control, an aliquot of suspended NPs was subjected to microwave-assisted digestion using a Discovery SPD Microwave Digester (CEM Corporation, USA). Briefly, 1.5 mL was diluted 2-fold with concentrated nitric acid, and digested at 210 ºC, using a ramp to temperature organic pressure mode (400 psi), with a ramp time of 4 minutes, a hold time of 15 minutes, at 450 W, with medium stirring.

After cooling to room temperature, digested samples were diluted with Milli-Q water to obtain a final nitric acid concentration of 2% for ICP-MS analysis.

For determination of total metal concentration ICP-MS was utilized. A calibration curve for the metal of interest was generated with the following concentrations: 0, 1, 5, 10, 50 µg/L. The solutions of interest were diluted accordingly to be within the range of the

standard curve. KED mode was used with a 0.1 s dwell time, with scandium used as an internal standard.

2.2.7 Submerged mammalian cell culture and CuONP exposure

All cells used in this study were maintained at 37 ºC in a humidified 5% CO_2 atmosphere. A549 human lung epithelial cell lines from ATCC were cultured in RPMI 1640, supplemented with FBS (10%), penicillin (600 µg/mL) and streptomycin (100 µg/mL). For submerged conditions, cells were seeded onto polystyrene culture dishes with 2 mL of media. For submerged experiments, CuONP powder was diluted to 0.1 mg/mL in media, and sonicated at 60 Hz for 5 minutes to ensure complete dispersion. The appropriate dilutions in media were made, and 2 mL was added to the cells for up to 24 h prior to the start of experiments. For CuONPs exposures involving pre-treatment with a drug, cells were exposed to the appropriate drug 1 h prior to CuONP exposure. For subsequent experiments with bacteria, exposure to CuONPs was performed in antibiotic-free RPMI 1640 media.

2.2.8 alamarBlue assay

Cell viability of NP-exposed cells was determined using the alamarBlue assay, which directly measures the conversion of the non-fluorescent resazurin to the highly fluorescent resofurin at 570 nm. This reaction is dependent on a functioning mitochondria, which correlates with cell viability. In brief, alamarBlue was diluted 15-fold in media, and 0.5 mL was added to NP-treated cells. Cells were incubated at 37 ºC and the absorbance at 570 nm and 600 nm was measured at the specified times to observe reduction over time.

2.2.9 Generation of reactive oxygen species (ROS)

NP-treated A549 cells, cultured in 24 well dishes were washed twice with PBS and were incubated with DCFDA (10 μM final) in Hank's buffered saline solution (HBSS) for 1 h to allow for probe uptake and intracellular ester cleavage and oxidation into the green fluorescent product. Cells were washed twice with PBS and lysed in 300 μL of Triton X-100 (0.1% v/v) and shaken at 600 rpm for 5 minutes to ensure lysis and homogenization. The degree of oxidation was measured using a Synergy H1 Hybrid Multi-mode microplate reader (BioTek) by measuring the green fluorescence at 495/530 nm (excitation/emission).

2.2.10 Lipid peroxidation

NP-treated A549 cells were treated with C11-BODIPY$^{581/591}$ (2 μM final) without a media change 1 h before the end of NP exposure. This lipid fluorophore is rapidly incorporated into biological membranes where it is oxidized specifically by peroxy-radicals. This oxidation results in a shift from 590 nm (red) to 510 nm (green). Cells were washed twice with PBS and lysed in 300 μL of Triton X-100 (0.1% v/v) and shaken at 600 rpm for 5 minutes to ensure complete homogenization. The degree of peroxidized lipids was quantified using a Synergy H1 Hybrid Multi-mode microplate reader (BioTek) by measuring the loss and gain of red and green fluorescence, respectively.

2.2.11 Multiplex ELISA

Multiplex ELISA was done in accordance to the manufacturer's directions. Magnetic beads specific towards human IL-6, IL-8, and MCP-1 were used. A standard curve was also made using a series of beads corresponding to the cytokine, and diluted to 500 μg/mL with PBS. All incubations were protected from light. Briefly, samples were prepared by collecting the supernatant after CuONP exposure. Magnetic beads (50 μL)

were washed with 100 µL of assay buffer, followed by the addition of 50 µL of sample. The sample was incubated at 25 ºC for 30 minutes followed by three washes. This was followed by the addition of antibody and incubation for 30 minutes as before. Lastly, 50 µL of streptavidin-PE was added and incubated for 10 minutes. The beads were washed three times and analyzed using a Bio-Plex® 200 luminometer.

2.2.12 FACS analysis

Cells were stained using the Annexin V Apoptosis Detection kit. Briefly, NP-treated A549 cells were washed twice with 1X PBS, and collected in 0.25 mL trypsin-EDTA (0.25%). The trypsin was neutralized with 1 mL of media, and cells were subjected to centrifugation at 600 g for 5 minutes. Cells were washed once with 1X binding buffer (BB), then suspended in the same buffer at $5x10^5$ cells/mL. The cells were subjected to centrifugation at 600 g, and then resuspended in 195 µL BB with 5 µL Annexin V-FITC for 10 minutes. Cells were washed as before, and resuspended in 190 µL BB with 10 µL 7-AAD (5 µg/mL final). Samples were incubated for 5 minutes, and filtered through a nylon-mesh filter to remove cell aggregates. Cells that were subjected to 55 ºC for 30 minutes were used as a positive control in addition to negative and single-stained controls. Annexin V-FITC and 7-AAD signal intensities were measured using a CytoFLEX Flow Cytometer with appropriate laser configurations (Beckman Coulter, USA). The system was set to capture 20,000 events per treatment.

2.2.13 Selection of serotypes and culturing of S. pneumoniae

According to Wong et al. [14], there was increased prevalence of *S. pneumoniae* serotypes 4 and 8 in welders compared to the working-age population. Serotype 4 was chosen for initial experimentation, with extension to the other serotypes: 8, 23B, 7F, and

19A as needed as these serotypes are responsible for most of the vaccine-preventable pneumococcal disease in Canadian hospitalized adults.

2.2.14 Bacterial adherence assay

Two days prior to CuONP exposure, an inoculum of *S. pneumoniae* was cultured on a tryptic soy agar (TSA) plate supplemented with 5% sheep blood and cultured overnight at 37 ºC in a humidified 5% CO_2 atmosphere. From this plate, 5-6 colonies were chosen, and a bacterial lawn was grown on a new plate and grown overnight.

Taken from the bacterial lawn plate, *S. pneumoniae* was suspended in PBS and the optical density measured at 600 nm. Bacteria were subjected to centrifugation at 6000 RPM for 5 minutes and resuspended in RPMI media containing no antibiotics at a multiplicity of infection (MOI) of 10. This bacterial suspension was added to NP-treated A549 cells (0.5 mL) which had been washed twice with PBS. Adhesion was allowed to proceed for 2 h. Afterwards, A549 cells were washed three times with PBS to remove loosely attached pneumococci. Attached pneumococci were detached using 0.25 mL trypsin (0.25%) and A549 cells were permeabilized with 0.75 mL of saponin (0.1% w/v) to recover intracellular bacteria. The samples were serially diluted, grown on TSA plates, and cultured overnight at 37 ºC in a 5% CO_2 humidified atmosphere. Colonies were then counted 12 h later to determine total adhered bacteria.

2.3 CuONP exposure using an air-liquid interface (ALI) cell model

2.3.1 NP generation for ALI exposure

Nitrogen [(3.8 litres per minute (LPM))] was delivered to the NP generation chamber where a spark was formed between two metal electrodes and adjusted to 0.4 mA. The electrodes can be composed of a number of metals; however, copper (>99.9%)

electrodes were chosen. These freshly generated copper NPs were supplemented with O_2 (0.95 LPM) and 5% CO_2 (0.25 LPM) to mimic proper cell culture conditions before entering the InvitroCell exposure chamber where A549 lung cells were contained.

Each NP-exposed group was normalized and compared to a matched, unexposed control group for each experiment, called the "incubator control." Additionally, an air exposure was performed which consists of the above NP generation, but NPs were filtered out using a HEPA filter immediately prior to delivery (NP-free air).

All measurements and end-points are similar in method as compared to the submerged experiments, except where otherwise noted below.

2.3.2 Size distribution of NPs delivered at an ALI

Since the SMPS only uses 1.5 LPM, NP size and number can be quantified at the same time as NP delivery to cells. This allows for a consistent generation of NP size and number during the entire length of the exposure, and between exposures.

2.3.3 TEM of NPs delivered at an ALI

The procedures were the same as in Section 2.1.3, with the following modifications. NPs were generated as described previously in Section 2.2.2 and delivered onto a Formvar-coated copper TEM grid by electrostatic precipitation (towards anode) using a Nanometer Aerosol Sampler (TSI) for 24 h.

2.3.4 Cell culture and NP delivery for cells exposed at an ALI

Culture conditions for cells exposed at an ALI was the same as in Section 2.2.7, with the following changes. Instead, cells were seeded onto 0.4 μm polyester transwell membranes with 2 mL of media on the basal side, and 1 mL on the apical side. The apical

media was removed 12 h prior to NP exposure. For ALI experiments, transwell membranes without apical media were transferred to the exposure apparatus (InvitroCell) that contained 17 mL of basolateral media. Copper NPs were generated and delivered to cells within the InvitroCell.

2.4 Statistical analysis

Unless otherwise stated, each experiment is given as the mean and standard error of the mean (SEM) of at least three experiments, performed in duplicate. Significance was determined using a two-tailed t-test assuming unequal variances. The significance is shown as a *p*-value with <0.05 (*), <0.01 (**), <0.001 (***).

CHAPTER 3: RESULTS

3.1 Synthesis and characterization of CuONPs

Copper oxide nanoparticles (CuONPs) were synthesized using a simple one-step method, which involved heating a solution of copper (II) sulfate, and then promoting nucleation of NPs by adding NaOH. Particle size is largely dependent on the duration and temperature of the reaction, which can be manipulated as desired. The goal was an apparent size of 20-50 nm as these are the sizes used in other studies. To confirm the size, a solution of synthesized CuONPs was aerosolized using an atomizer, and analyzed using the size mobility particle sizer (SMPS). The particles were shown to have an apparent mean size of 30 nm, corresponding to approximately 2 x 10^6 particles/cm^3 **(Fig 3.1.1)**. The geometric standard deviation was less than 1.6, indicating a narrow range of particle sizes. However, the distribution was not completely normal as it exhibited slight positive skewness. This means that the distribution was concentrated towards the left of the graph (more smaller particles), but also had a longer tail indicating a small population of larger particles. But, since water itself can influence the apparent size distribution by overestimating the apparent size, it was necessary to perform a water correction. This means that the distribution graph for MilliQ water was subtracted from the CuONP distribution graph to obtain a final distribution.

It had been hypothesized that these CuONPs particles were spherical because the synthesis process involving NaOH usually yields spherical particles with other metals (eg: iron), and it was thought that copper would behave similarly as it belongs to the same family of transition metals (atomic number 26 for Fe; 29 for Cu). However, there are many chemical processes that govern nucleation kinetics, and therefore it can be difficult to

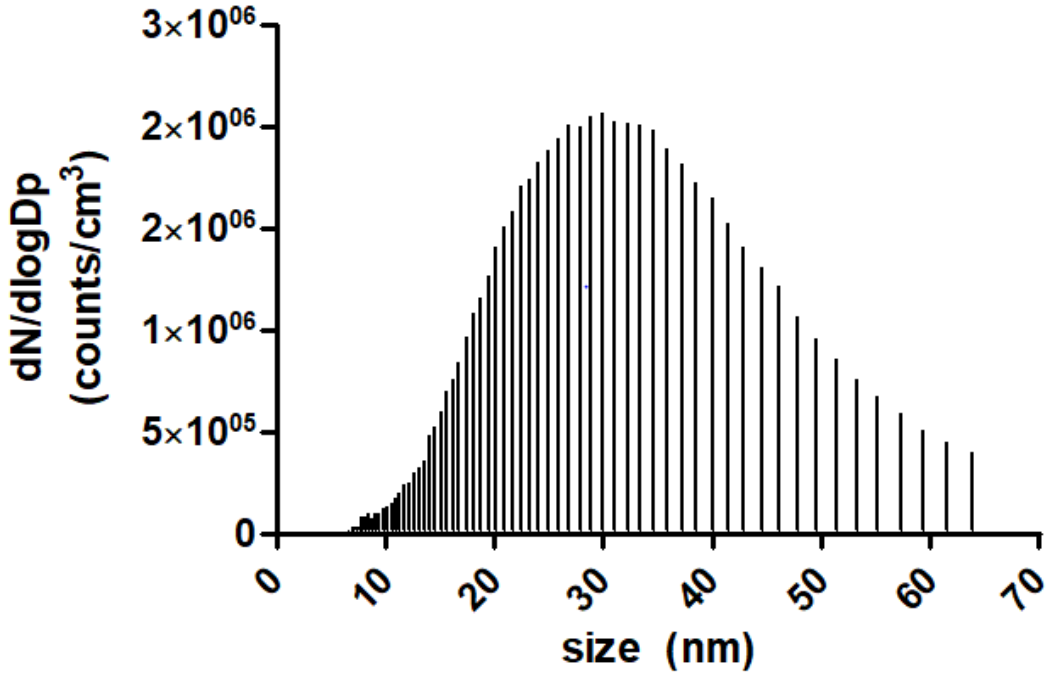

Figure 3.1.1. CuONPs have an apparent size of about 30 nm. NPs were suspended in MilliQ water to 0.1 mg/mL and sonicated at 60 Hz for 5 minutes to ensure complete dispersion. The solution was aerosolized using a TSI 3076 constant output atomizer and water vapour was removed using a TSI 3062 Diffusion dryer to obtain dried NPs. The size distribution of the dried particles was analyzed using a size mobility particle sizer (TSI 3085 or 3080) coupled to a condensation particle counter (TSI 3775), with a water correction applied.

predict the final size and shape. TEM was performed on the newly synthesized particles with adequate nanometer resolution **(Fig 3.1.2)**. Whereas iron NPs were spherical, with an approximate diameter of 30-50 nm (data not shown), CuONPs were not spherical. Instead, CuONPs exhibited a wire, or "rod-like" morphology, with a large length to width ratio. These particles seemed to cluster or "clump" together, giving a "shards of glass" appearance.

XRD is an analytical technique to determine the atomic arrangement and ultrastructure within the sample. In simple terms, XRD tells you the shape of your compound, and provides more detailed chemical evidence as compared to TEM or SMPS. When subjected to diffraction, CuONPs had high similarity to CuO nanowires characterized elsewhere **[145,146] (Fig 3.1.3)**. It was not a 100% overlap, but it was high enough that it could be concluded that these particles were wire- or rod-shaped. This agreed with the TEM data. Moreover, XPS was done to determine the elemental composition of the NPs **(Fig 3.1.4)**. This is because the outer layers of copper NPs can be oxidized, which could affect its toxicity. Also, copper oxides can exist in either the cuprous (Cu^{+}) or cupric (Cu^{2+}) forms, and this could affect the dissolution rate. It was shown that these synthesized particles were mostly cupric with a 2+ oxidation state, and that there were a lot of hydroxyl (-OH) groups. This is not surprising because the rod-like morphology of these CuONPs would result in a large surface area to volume ratio as compared to a more spherical particle.

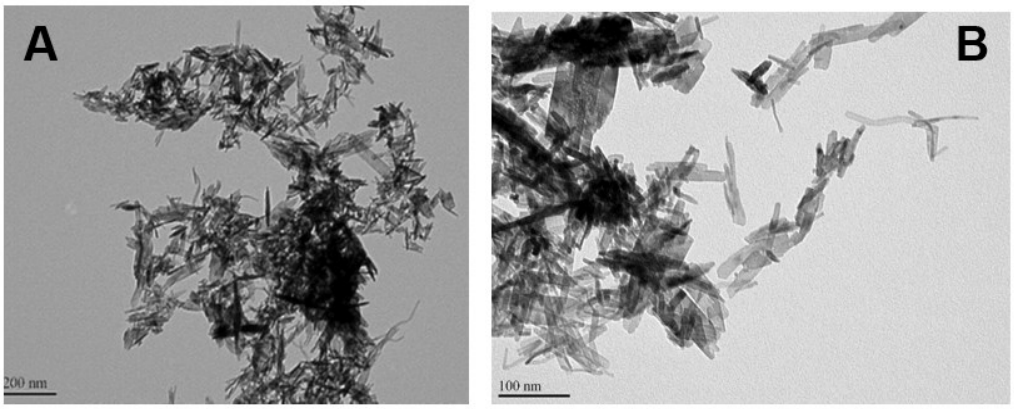

Figure 3.1.2. CuONPs have a rod/wire like morphology. CuONPs were suspended in absolute ethanol to 0.1 mg/mL and sonicated at 60 Hz for 5 minutes. The solution was added dropwise to Formvar-coated copper TEM grids allowing for evaporation between each drop. Grids were analyzed with a FEI Technai-12 transmission electron microscope in order to determine the size and morphology of the copper NPs. Size markers are given as either 200 nm **(A)** or 100 nm **(B)**.

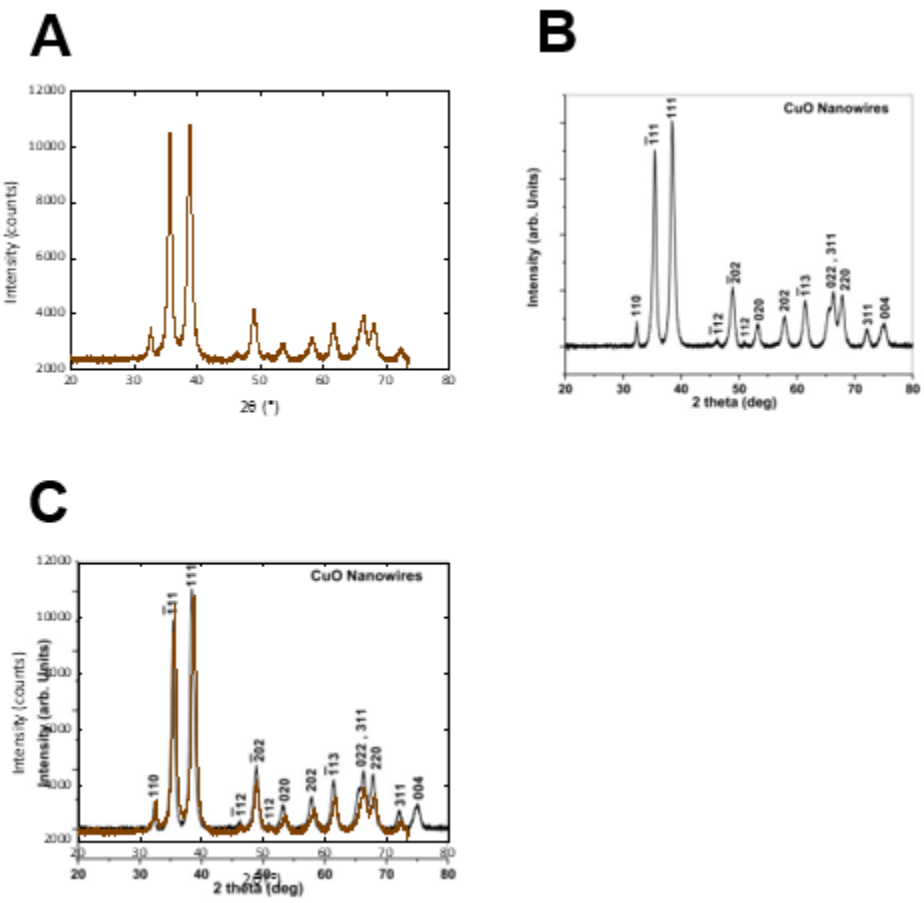

Figure 3.1.3. CuONPs have a near nanowire-like structure. CuONPs were deposited onto an XRD well-plate, and data was collected using a JD2000 diffractometer equipped with a Cu target X-ray tube and a diffracted beam monochromator. The generator was set for 40 kV and 30 mA. Data was collected between 2Θ = 20° and 75° at 0.02° intervals. The count time was 8 s per point, giving a total scan time of 7 h **(A)**. Data was compared to CuONP nanowires synthesized independently from another lab (Ethiraj, 2012) **(B)**. For emphasis, data was overlayed to show similarity of samples **(C)**.

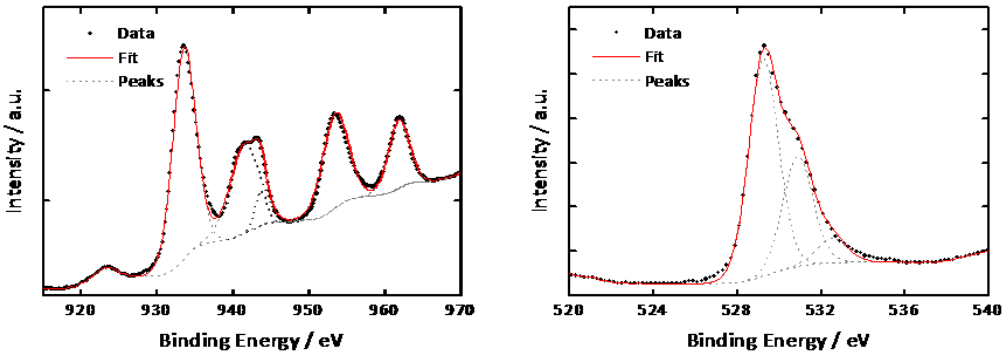

Figure 3.1.4. XPS confirms CuONPs with a 2+ oxidation state. CuONPs were submitted to the Dalhousie Physics Department and analyzed using a Multilab 3000 XPS system. The data was collected with a dual anode X-ray source using MgKα irradiation.

It is important to fully understand the physiochemical properties of a nanoparticle as this will help to better predict and explain toxicological outcomes. For example, dissolution of CuONPs into Cu^{2+} ions is required for toxicity. It then follows that a more rapid dissolution would lead to a more rapid and acute toxic response than a slower (or no) dissolution. A549 cells were used to observe whether they affected the rate of CuONP dissolution and copper ion concentration was measured using ICP-MS **(Figure 3.1.5).** Some NPs have been shown to require intracellular compartmentalization for complete dissolution (acting like a Trojan Horse) and whether a similar effect could be observed with CuONPs was unknown. However, when the media and cells were analyzed for copper ion concentration at 24 h post exposure it was found that most copper was found in the extracellular media, and not within cells **(Fig 3.1.5A).** The balance of copper was assumed to be as a non-dissoluted NPs, and this was found to make up a very small portion of the total copper. In other words, most of the CuONPs had dissoluted into copper ions. However, it was still possible that cells still contributed to dissolution, with rapid elimination, secretion from the cell or by cellular lysis during cell death. To measure this, a 24 h time-course of CuONPs in media with and without cells was completed **(Fig 3.1.5B)**. It was found that 1) dissolution was the same with and without cells suggesting that dissolution is not dependent on cell compartments or cellular processes, and 2) dissolution is very rapid, with almost 100% dissolution by 3 h. Taken together, this suggests that CuONP treatment may lead to an acute, rather than a chronic toxic response since cells would be met with a large bolus of toxic ions during a short period of time.

As mentioned above, CuONP dissolution into copper ions is rapid in media (RPMI 1640). Although significant, this may not necessarily be the most representative of true

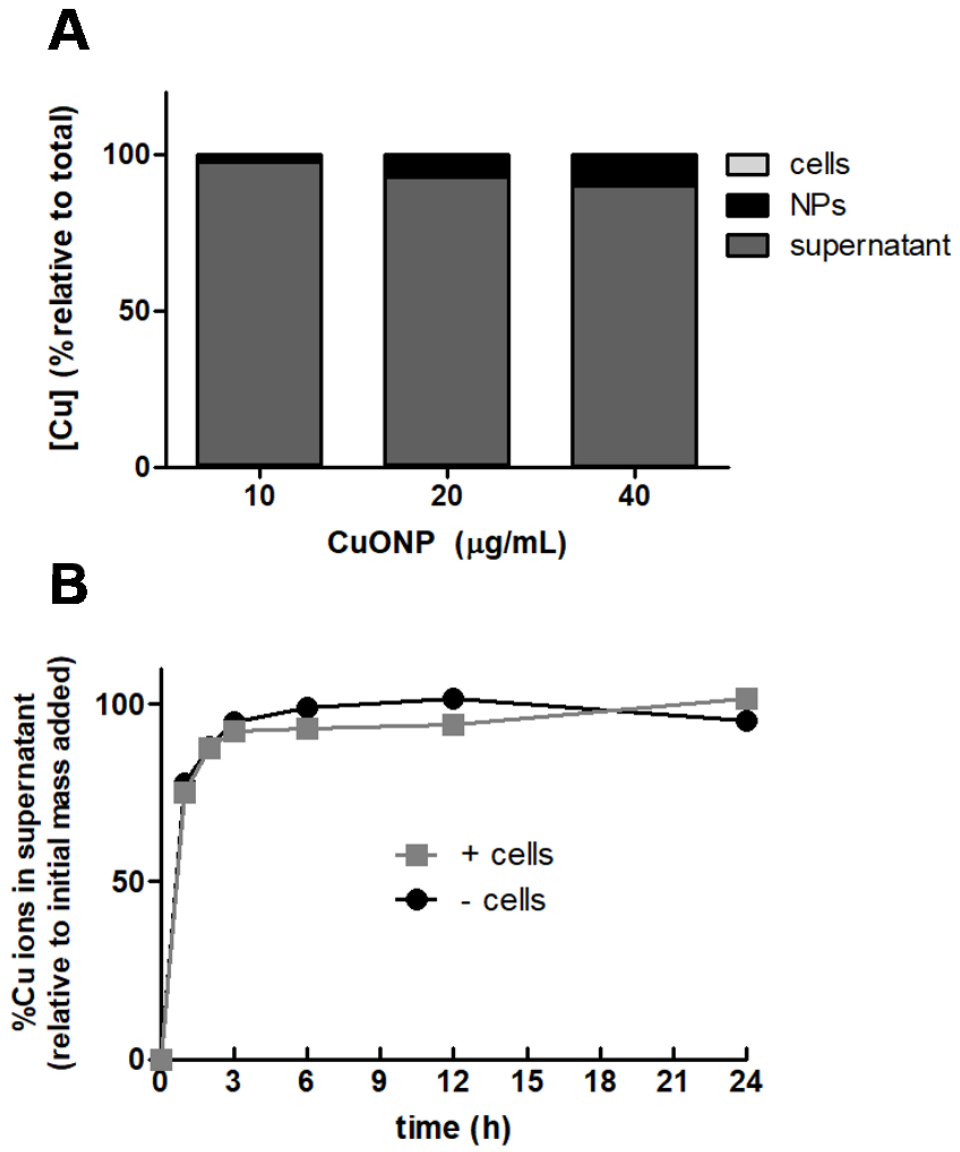

Figure 3.1.5. A549 cells do not affect the rate of CuONP dissolution. A549 cells were incubated with increasing concentrations of CuONPs for the indicated times. At 24 h CuONP exposure, media was collected, subjected to centrifugation, and filtered to remove undissoluted NPs. Cell pellets were subjected to microwave-assisted digestion. Solutions were diluted accordingly with HNO_3 and analysed using ICP-MS. Using a total digested 100% control , the percent of undissoluted NPs was inferred **(A).** CuONPs were added to dishes with or without cells, and the supernatant was collected at the indicated times, and Cu ion concentration was measured as before **(B).** Results are given as the mean and SEM of one independent experiment done in duplicate.

dissolution kinetics. In other words, it was not known whether there was something special about RPMI media that facilitates dissolution that may not be observed in other solutions. To test this, a 3 h time course of CuONP dissolution in media and water (Milli-Q) was completed **(Fig 3.1.6A).** It was found that NPs in media reached about 70% dissolution within 1 h, with almost 100% dissolution by 3 h. On the other hand, water only had about 25% dissolution at 1 h, with only 30% dissolution by the full 3 h. It is unknown whether CuONPs in water would reach 100% dissolution given enough time (eg: 24 h+) or would simply reach an equilibrium point much lower.

RPMI media [pH 7.4] contains many growth factors and supplements required for cells to grow which water does not contain. Each media component could be removed and dissolution reanalyzed, but this was not logical or practical to do. Rather, fetal bovine serum (FBS) was omitted simply because it makes up a large percentage of the finalized media (10%). CuONP dissolution was measured in media containing FBS, without FBS, and Milli-Q water using ICP-MS **(Fig 3.1.6B).** It was found that dissolution was similar in the media with and without FBS, suggesting that FBS does not affect CuONP dissolution.

Although RPMI media [pH 7.4] is used to culture human A549 lung cell lines, it may not be completely representative of normal lung physiology, where lung cells are in contact with other solutions, which may or may not affect CuONP dissolution kinetics. To measure this, CuONP dissolution was measured in an artificial lysosomal fluid (ALF) (to mimic low pH lysosomes), a Gamble's solution (to mimic lung extracellular milieu), PBS and water were also used **(Fig 3.16C)**. It was found that dissolution was the same in media as ALF (pH = 4.5) and Gamble's solution (pH 7.3) suggesting that pH does not affect rate of dissolution. On the other hand, CuONPs in PBS (pH 7.4) had no dissolution, even lower

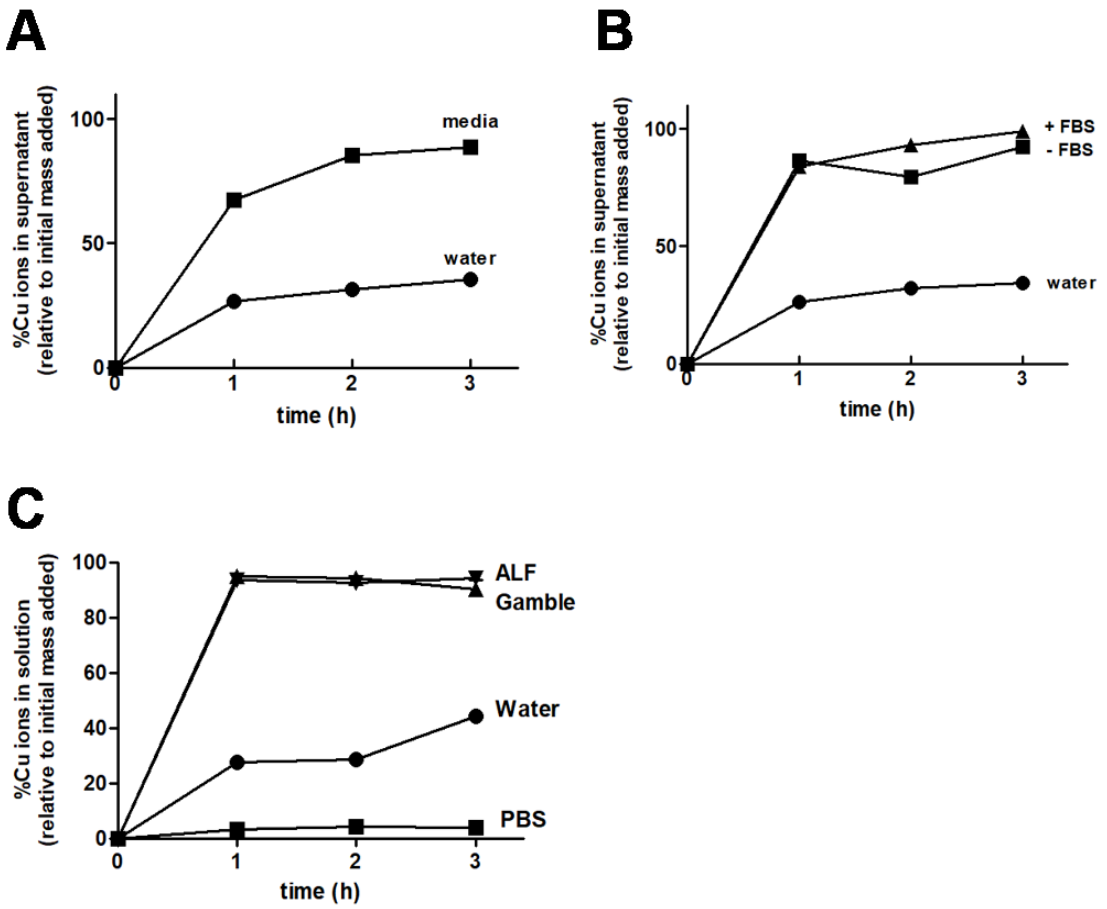

Figure 3.1.6. CuONP dissolution rate is affected by solution composition. CuONPs were incubated at 37 ºC in RPMI media containing FBS **(A,B)**, RPMI media without FBS **(B)**, and ALF, Gamble's and PBS **(C)** for the indicated times. Milli-Q water was used as a comparator. Solutions were collected, subjected to centrifugation, and filtered to remove undissoluted NPs. Solutions were diluted accordingly with HNO_3 and analysed using ICP-MS. A total microwave-assisted digested control was used to indicate 100% dissolution. Results are given as the mean and SEM of one independent experiment done in duplicate.

than that of water [pH 7]. Taken together, it is likely that there is a component in the RPMI media, ALF and Gamble's solution that facilitates CuONP dissolution.

3.2 The toxic potential of synthesized CuONPs

Previous research has shown that copper NPs are toxic to many different cell types. However, since my synthesized NPs are quite novel, it is still important to establish a toxicity profile of these NPs. A549 cells were treated for 24 h, with different concentrations of CuONPs, ranging from 0.3 μg/mL to 40 μg/mL. Based on simple observations using a light microscope, CuONPs were shown to be toxic starting at around 10 μg/mL, based on the finding of fewer cells, of which were no longer in firm contact with the culture dish **(Fig 3.1.7A)**. At lower CuONP concentrations (5 μg/mL), cells appeared very similar to untreated cells suggesting that toxicity of CuONPs may require a minimum threshold dose. Although light microscopy can provide rapid indication of cellular health, concrete conclusions should not be drawn from it as it provides no mechanism for toxicity. To determine whether there were changes in cell proliferation and cell viability after CuONP exposure, a commercial alamarBlue assay was used. Indeed, cell viability was monitored over a 4-hour time course to gauge the linearity of alamarBlue reduction in untreated and CuONP-exposed cells. **(Fig 3.1.7B)**. At 5 μg/mL, viability was similar to untreated cells which agreed with morphological observations from before. However, as the dose of CuONPs increased, there was a concomitant decrease in cell viability. At 10 μg/mL cell viability was approximately 70% as compared to control. At 20 μg/mL and 40 μg/mL, viability was less than 50% and 20%, respectively.

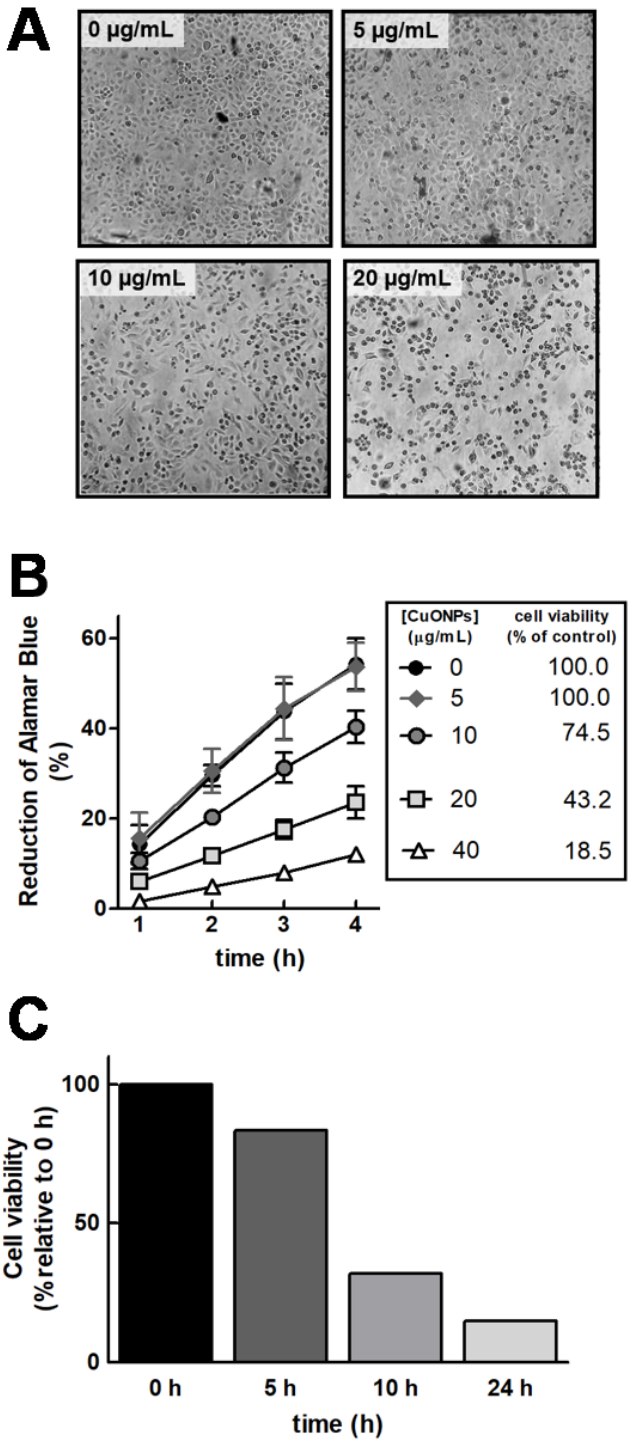

Figure 3.1.7. Increasing CuONP concentration results in decreased cell viability. A549 cells were cultured with CuONPs for the indicated times. Cells were observed for changes in cell morphology using a light microscope at 24 h **(A)**. Cell viability after increasing CuONP concentrations was measured using an alamarBlue proliferation assay at 24 h **(B)** and earlier time points with 20 µg/mL **(C).** The values presented are the mean and SEM of two (B) or one (C) independent experiment(s) done in duplicate.

Although a dose-response relationship has been established, it is important to determine whether toxicity increased as duration of exposure increased. It was hypothesized that a longer exposure would lead to a concomitant decrease in cell viability. Indeed, at a fixed 40 μg/mL dose, cell viability was approximately 90%, 35%, and 20% at 5 h, 10 h, and 24 h, respectively. It is important to note that this decreased cell viability is not linear, with what appears to be an initial lag phase that could be attributed to the fact that it took time for complete dissolution of the particle into toxic Cu^{2+}. Nonetheless, CuONPs can be considered acutely toxic.

Oxidative stress, generation of free radicals and reactive oxygen species (ROS) are major events that ultimately govern the fate of the cell. If the oxidative stress and inflammation is low enough, the cell can overcome this by upregulating its antioxidant capacity, which would be a good to do as a future experiment. On the other hand, if the stress is too high, this will promote cell death. Oxidative stress was measured by incubating CuONP-exposed cells with a fluorescent probe that is oxidized by intracellular ROS to give a green fluorescent product **(Fig 3.1.8A)**. At 20 μg/mL there was a modest 30-40% increase in ROS levels as compared to control. At 40 μg/mL, ROS levels were about 50-60% higher than control. CuONP exposure and ROS generation does not appear to exhibit a dose-response relationship at the concentrations and timepoints assessed..

Since copper ions are found primarily extracellular, it was thought that intracellular ROS levels may not be completely indicative of a true stress response. As a result, a more stable extracellular indicator of oxidative stress was measured. Plasma membranes are enriched in lipids that are oxidized in the presence of peroxy-radicals generated through

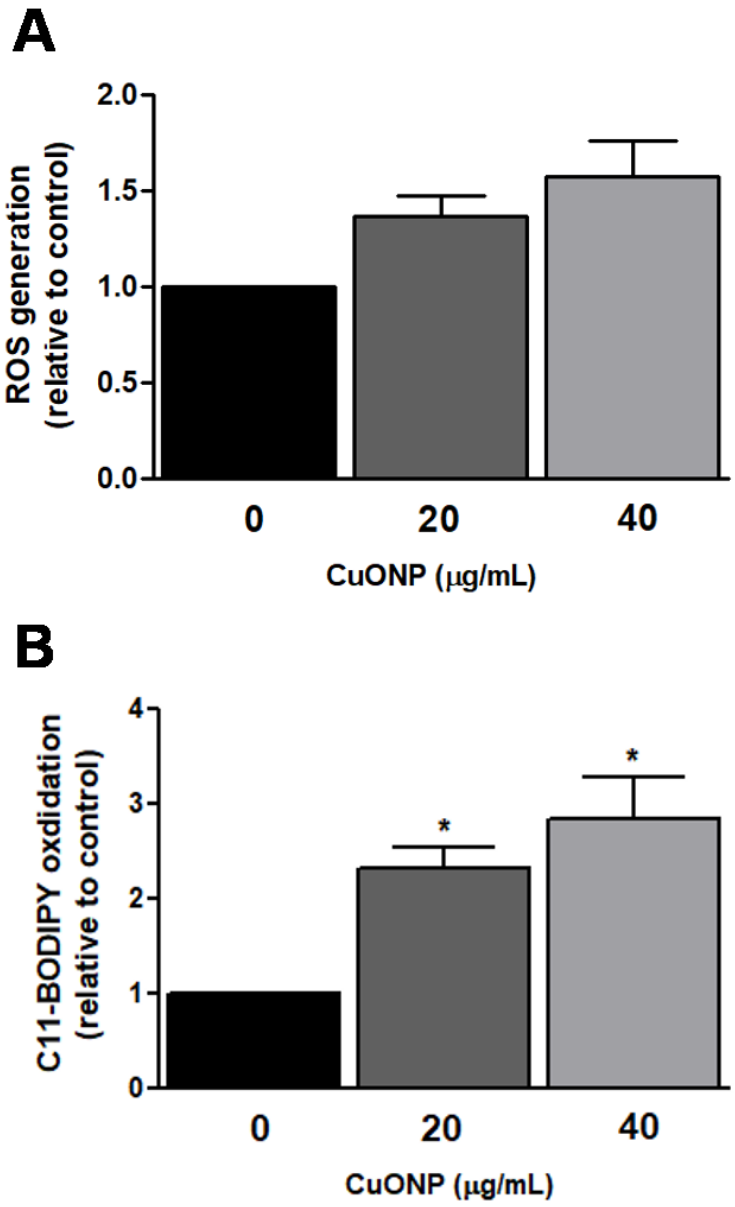

Figure 3.1.8. ROS generation and lipid peroxidation is increased after CuONP exposure. A549 cells were treated with increasing concentrations of CuONPs for 24 h. Cells were incubated with a DCFDA probe (5 μM), permeabilized with Triton X-100 and fluorescence (green) was measured at 495/530 nm **(A)**. Cells were incubated with C-11 BODIPY (2 μM) for 30 minutes, permeabilized with Triton X-100, and fluorescence measured at 581/591 nm and 488/510 nm **(B)**. Results are given as the mean and SEM of three independent experiment done in duplicate. Controls are given as the ratio of absorbances corresponding to no CuONP addition.

oxidative stress. The degree of lipid peroxidation was measured by monitoring the incorporation and oxidation of a C-11 BODIPY$^{581/591}$ probe into membranes **(Fig 3.1.8B)**. Indeed, at 20 μg/mL, and at 40 μg/mL CuONP there was a 2-fold, and 3-fold increase in lipid peroxidation, respectively. Taken together, CuONP exposure results in induction of oxidative stress which includes lipid peroxidation and generation of intracellular ROS.

CuONPs exhibit rapid dissolution, acute toxicity; characterized by decreased cell viability and ROS generation. Since iron is a major component of welding fumes and combustion emissions, it was wondered whether FeNPs exhibited a similar toxicological profile compared to CuONPs **(Fig 3.1.9)**. When A549 cells were treated with high concentrations of FeNPs (up to 10-fold higher than the highest CuONP dose) there was no change in morphology (**Fig 3.1.9A)**. Rather, FeNPs aggregated to form precipitates, which were clearly visible without the use of a microscope. This suggested that FeNPs may not experience dissolution at the same rate as CuONPs. Indeed, FeNPs were not shown to experience dissolution (~2-3%) in RPMI media after 3 h of incubation using ICP-MS **(Fig 3.1.9B).** Not surprisingly, there was no change in cell viability **(Fig 3.1.9C)** or lipid peroxidation **(Fig 3.1.9D)** further suggesting that FeNPs are not toxic to A549 cells, even at high concentrations. These results are in accordance with the hypothesis that NPs require dissolution to be toxic.

Since oxidative stress induces pro-inflammatory pathways such as NF-kB, it was also hypothesized that CuONPs would lead to production of pro-inflammatory cytokines and chemokines. As a result, production of IL-6, IL-8 and monocyte chemoattractant protein-1 (MCP-1) were measured. This was accomplished using a multiplex ELISA using

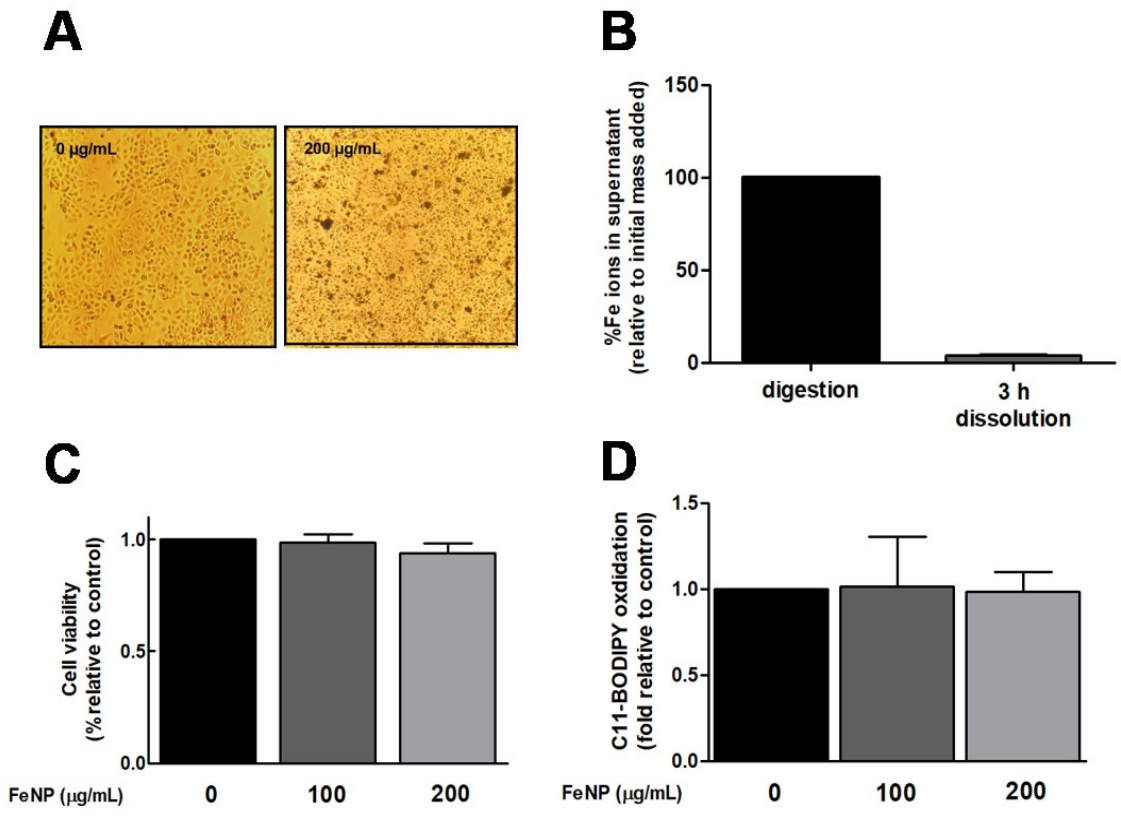

Figure 3.1.9. FeNPs do not result in cytotoxicity in A549 cells. A549 cells were treated with FeNPs for the specified times. Cell morphology and FeNP aggregation were visualized using light microscopy **(A)**. FeNPs (20 µg/mL) were incubated at 37 ºC for 3 h, subjected to centrifugation, filtered and Fe ion concentration analyzed using ICP-MS. A total microwave digestion of the same solution served as a control **(B)**. A549 cells were treated with increasing concentrations of FeNPs for 24 h with cell viability and lipid peroxidation measured using an alamarBlue assay, and C-11BODIPY$^{581/591}$ oxidation, respectively **(C, D).** The values presented are the mean and SEM of one experiment done in duplicate.

fluorescent beads corresponding to the cytokines of interest **(Fig 3.1.10)**. The concentration of CuONPs (20 μg/mL) was chosen as too much of an acute toxic response would result in out-right killing of cells, without a change in the inflammatory phenotype. Indeed, IL-6 levels were significantly increased, corresponding to an approximate 30% increase in IL-6 in the supernatant **(Fig 10A).** A similar response was achieved with IL-8, with an approximate significant increase of about 10% **(Fig. 10B)**. Removing the outlier in the IL-8 untreated group resulted in an IL-8 increase of 13%. Lastly, MCP-1 was shown to have increased by 3% after CuONP exposure **(Fig 10C)**. Although there was only a small increase in MCP-1 levels, the assay was sensitive enough, and the standard deviation was low enough to show significance of increased MCP-1.

The results collected so far indicate that CuONPs are toxic to A549 cells, where they induce oxidative stress, increase production of pro-inflammatory cytokines, ultimately leading to decreased cell viability. This decreased viability can be attributed to either reduced cellular metabolism (quiescence) or induction of cell death responses. It is hypothesized that cells are undergoing cell death since the characteristics of cell death, such as fewer cells and cell rounding is evident by light microscopy. Cell death can occur via two main pathways: apoptosis and necrosis. To differentiate between the two, flow-assisted cell sorting (FACS) was performed using Annexin-V and 7-AAD stains (**Fig 3.1.11A)**. After the appropriate gating was performed, there was clear evidence of a cell population shift from the bottom left, to the top left. This corresponds to a shift from a healthy population to a more necrotic population of cells after CuONP exposure. Moreover, there was no significant apoptotic population. Indeed, we see a dose-dependent increase in

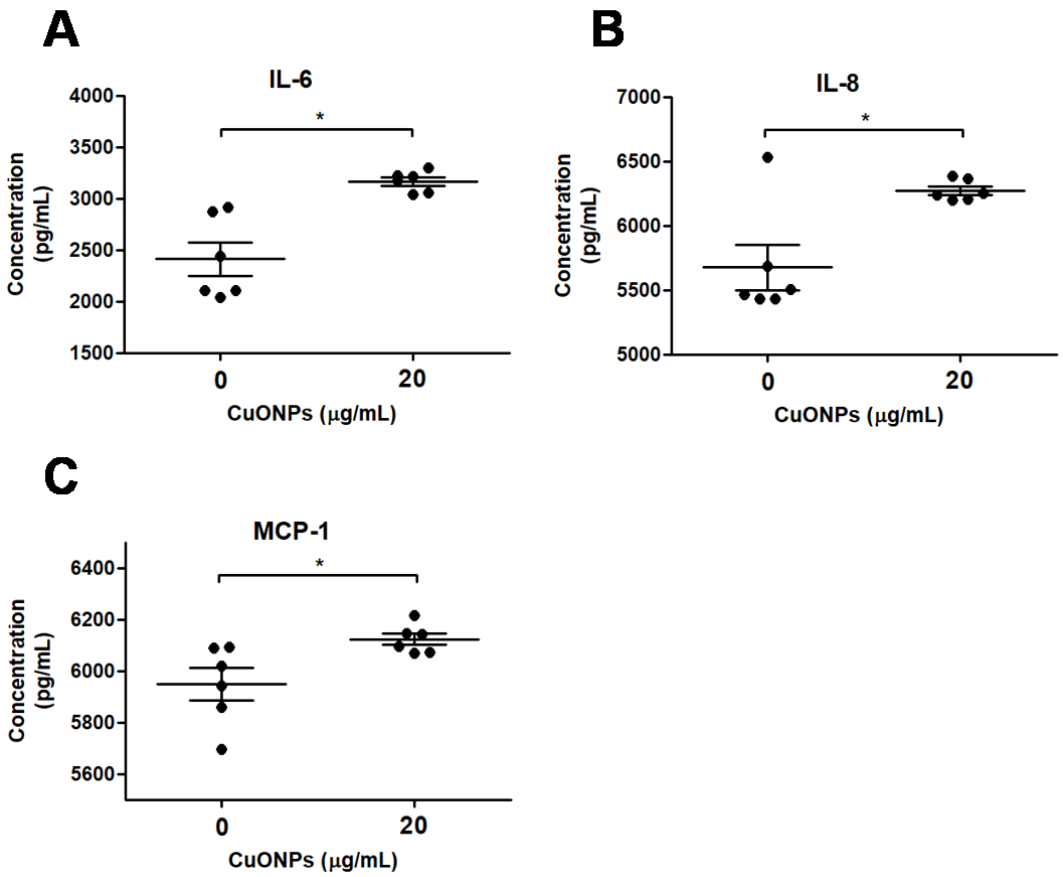

Figure 3.1.10. CuONP treatment results in production of inflammatory cytokines. A549 cells were treated with CuONPs (20 µg/mL) for 24 h. Cells were collected and subjected to multiplex ELISA using the appropriate beads corresponding to IL-6 **(A)**, IL-8 **(B),** or MCP-1 **(C)** and analyzed using a Bio-Rad Bio-Plex 200 system. Results are the mean and SEM of one experiment done in sextuplicate. * $P < 0.05$ using a student's *t*-test assuming unequal variances.

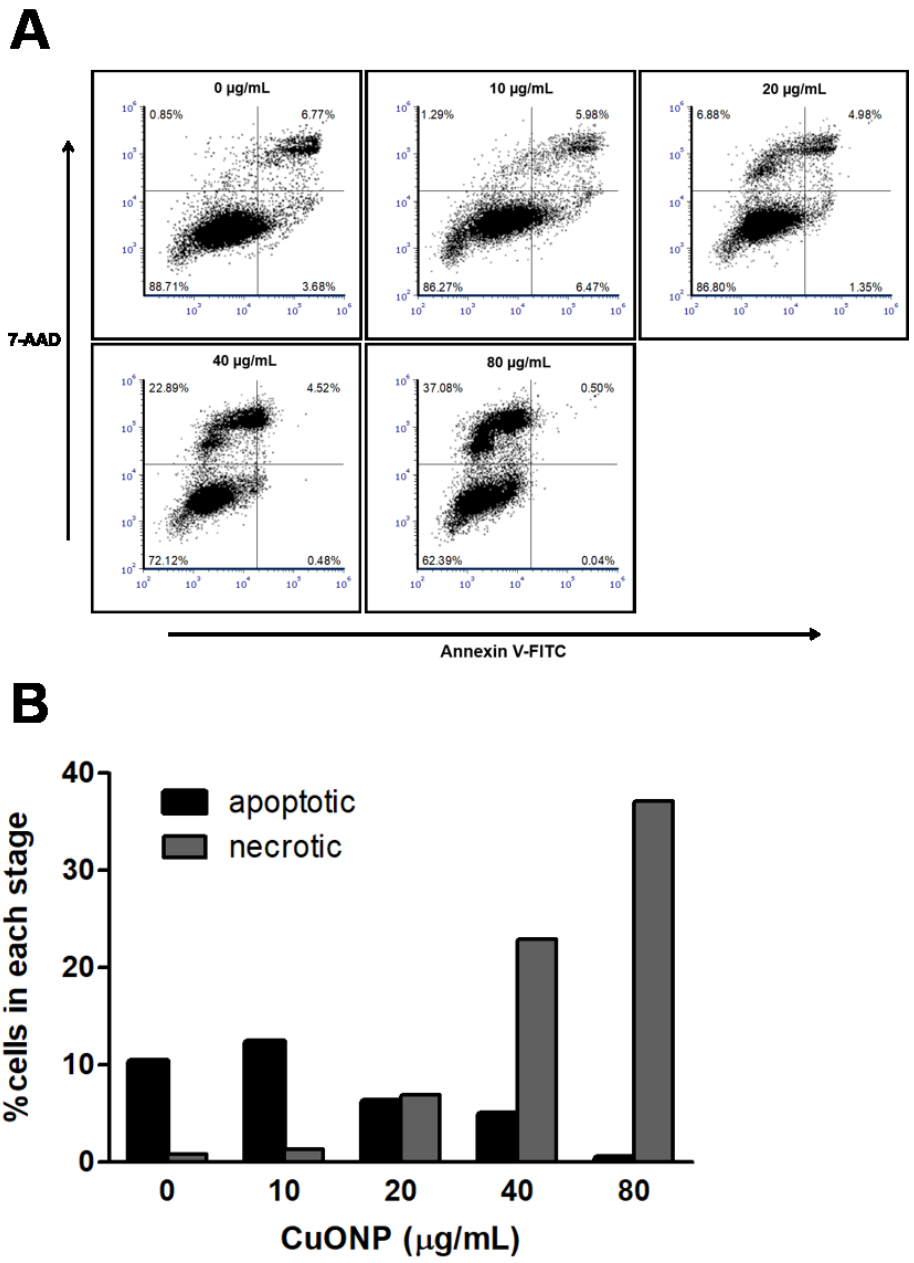

Figure 3.1.11. Necrosis is increased after CuONP treatment. Cells were incubated with increasing concentrations of CuONPs for 24 h. Cells were harvested, stained with Annexin V-FITC and 7-AAD in binding buffer and flow cytometry analysis was completed using a Beckman Coulter CytoFLEX with appropriate gating **(A).** The proportion of necrotic cells and apoptotic cells relative to the total population is also shown **(B).** Results are given as the mean and SEM of one independent experiment done in duplicate.

the number of necrotic cells after CuONP exposure (**Fig 3.1.11B)**. Although there appears to be apoptosis occurring at lower doses (10 μg/mL), it was not much different than the untreated control and therefore assumed to not be in response to CuONP treatment itself. Nonetheless, it appears as though necrosis is the favored cell death mechanism in response to CuONP treatment.

3.3 S. pneumoniae adhesion after NP exposure

It was hypothesized that *S. pneumoniae* would adhere more easily to A549 cells after treatment with CuONPs in a dose-dependent manner. In other words, it was thought that cell death causes a dose-dependent increase in adhesion of *S. pneumoniae.* To investigate this, CuONP-treated A549 cells were incubated with serotype 4, and adhered/internalized bacteria were collected, plated, and counted to determine adhered bacteria **(Fig 3.1.12A)**. The 2.5 and 5 μg/mL treatments resulted in little *S. pneumoniae* binding, and were similar to the control. However, the 10 μg/mL treatment had 3-fold more *S. pneumoniae* adhesion compared to untreated, and this increased to ~ 5-fold in the 20 and 40 μg/mL groups. Since there were fewer A549 cells in the high CuONP concentration groups, a negative control was done with *S. pneumoniae* added to plastic dishes with no cells to rule out non-specific binding (results not shown). It was thought that there could be something specific with serotype 4 that made it adhere better to CuONP-treated cells, so an assay using different serotypes was done to see if results were capsule-specific **(Fig 3.1.12 B)**. All serotypes had a similar dose-dependent increase in *S. pneumoniae* binding after CuONP exposure, but not all to the same effect. For example, serotype 8 had much lower adhesion, as compared to 23B, 7F, and 19A. Taken together, *S. pneumoniae* adhered

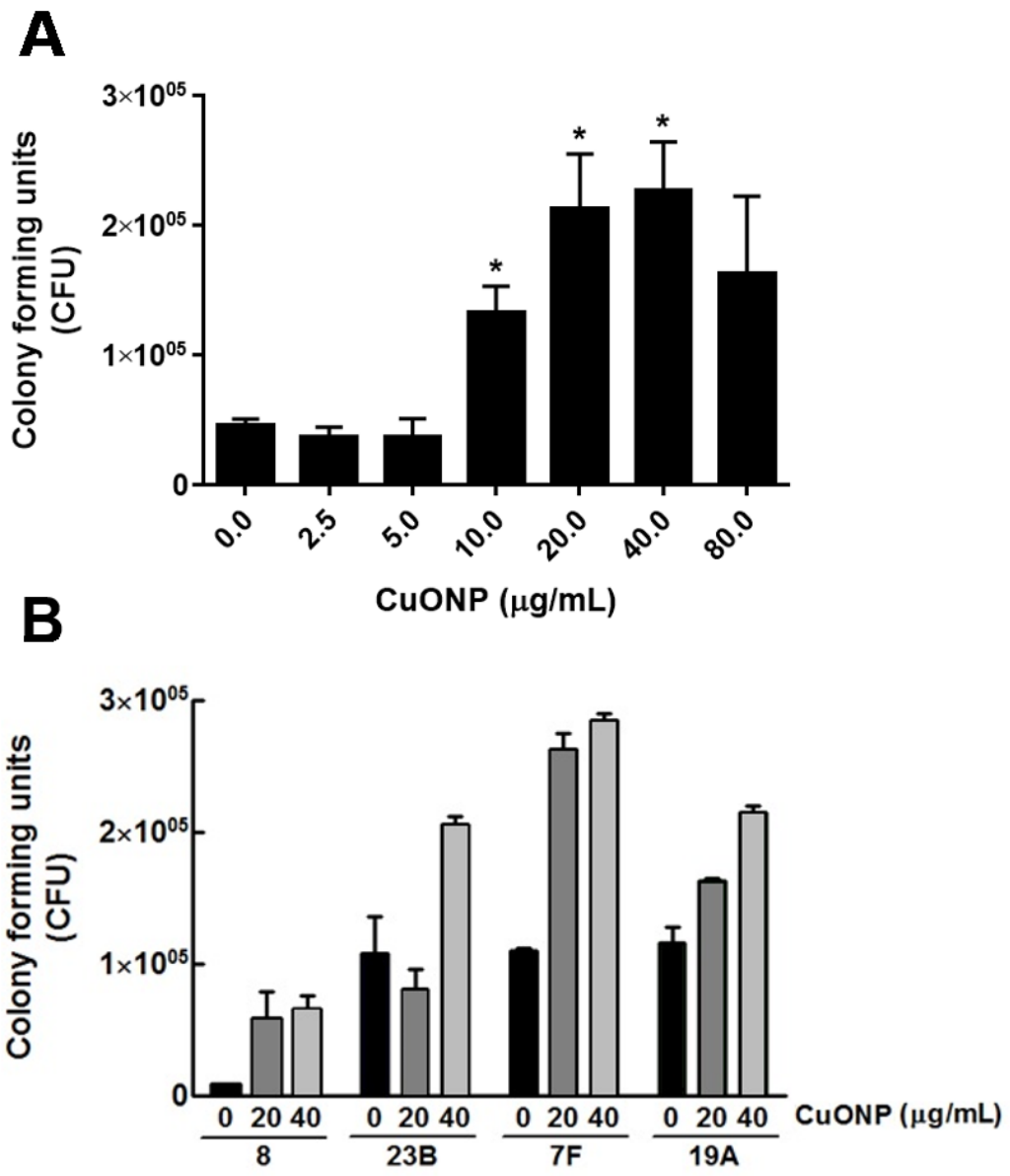

Figure 3.1.12. Adhesion of *S. pneumoniae* to human lung A549 cells is enhanced following exposure to CuONPs. A549 lung cells were exposed to CuONPs for 24 h. This was followed by incubation with *S. pneumoniae* serotype 4 **(A)** or 8, 23B, 7F, and 19A **(B)** at an MOI of 100 for 2 h. Afterwards, the cells were washed, trypsinized for 5 minutes, and lysed with saponin. Serial dilutions were made and 100 μL of each were streaked onto soy tryptic 5% sheep blood agar plates and cultured overnight at 37ºC in a humidified 5% CO_2 atmosphere. Colony forming units (CFU) were counted, and CFU/mL was determined. Results are the mean and SEM of three (A) or one (B) independent experiment(s). * $P < 0.05$ using a student's *t*-test assuming unequal variances.

more strongly to CuONP-treated A549 cells, and this is not thought to be capsule-specific.

Since oxidative stress and lipid peroxidation were increased after CuONP treatment, it was hypothesized that pre-exposure to antioxidants would decrease ROS to prevent induction of cell death responses. To test this, A549 cells were pre-incubated with increasing concentrations of N-acetyl cysteine (NAC) before being exposed to 20 μg/mL CuONPs. This was followed by an alamarBlue assay to measure cell viability **(Fig 3.1.13)**. Pre-treatment with NAC lead to a dose-dependent rescuing of cell viability after CuONP treatment **(Fig 3.1.13A).** Cell viability was about 30% without NAC and approximately 90% in the presence of NAC during CuONP treatment. However, NAC itself leads to increased cell viability in the absence of CuONPs and therefore any increases in cell viability after NAC and CuONP treatment may not be solely a result of ameliorating CuONP toxicity. To account for this, each NAC group was normalized to their respective "no CuONP control" **(Fig 3.1.13B).** When this correction is applied, we see that NAC still resulted in a dose-dependent increase in cell viability that can be directly attributed to the mitigation of CuONP toxicity.

Increased *S. pneumoniae* adhesion after CuONP exposure is hypothesized to be the result of increased cell death since more cell death is observed as CuONP concentration increases. Since NAC serves to increase cell viability after CuONP exposure, it was posited that NAC would lead to decreased adhesion of *S. pneumoniae*. When CuONPs were added to A549 cells and then challenged with *S. pneumoniae*, we observed the predicted increased pneumococcal adhesion as observed before **(Fig 3.1.14)**.

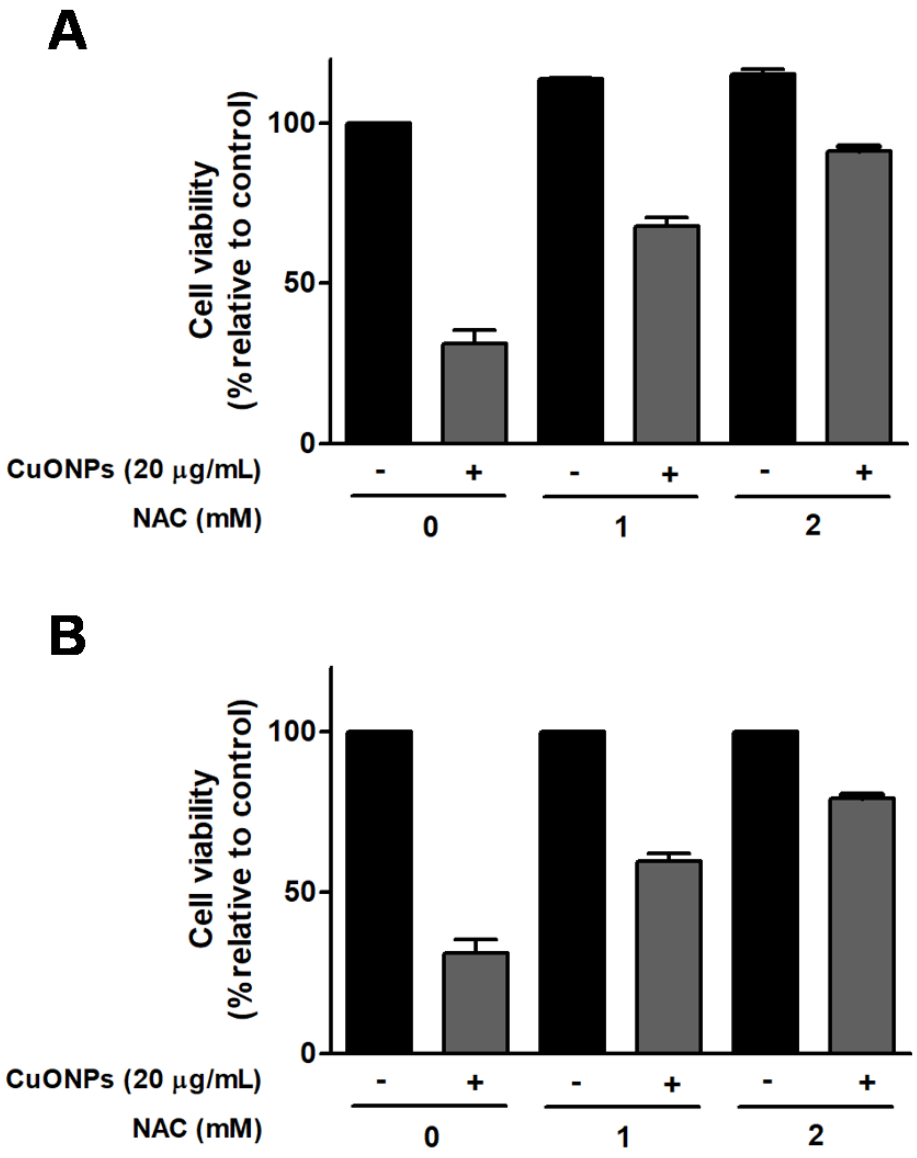

Figure 3.1.13. NAC restores cell viability caused by CuONP exposure. A549 cells were pretreated with increasing concentrations of NAC prior to exposure to 20 μg/mL CuONPs for 24 h. Cell viability was measured using an alamarBlue proliferation assay as previously described **(A and B).** To control for NAC effects on cell viability, all data was normalized to the "no NAC/no CuONP control" **(A)** or each NAC treatment individually to their respective "no CuONP control" **(B)**. Results are the mean and SEM of one experiment done in duplicate.

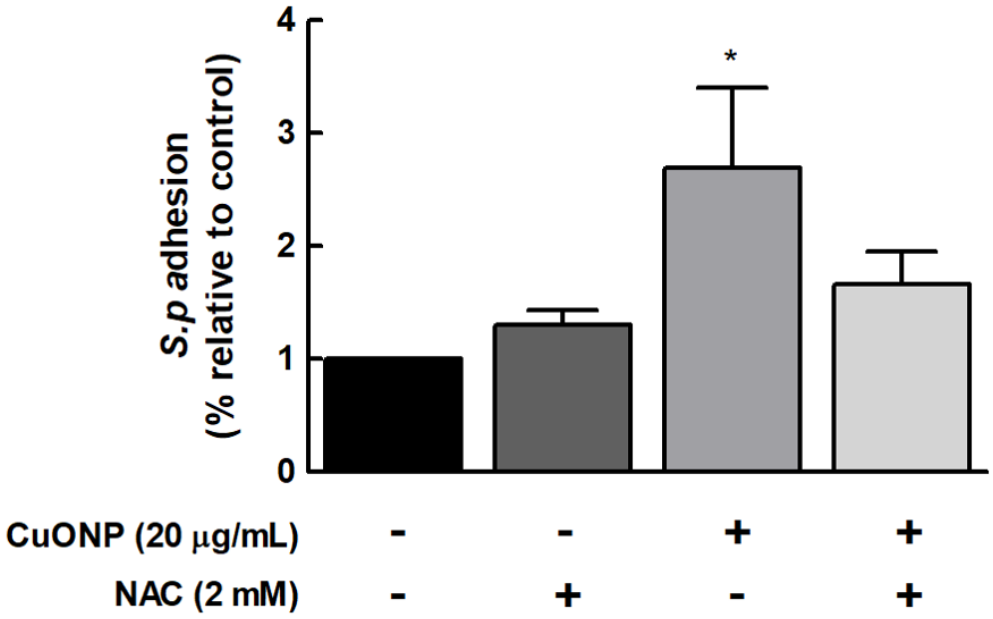

Figure 3.1.14. NAC pre-treatment prior to CuONP exposure is associated with decreased adhesion of *S. pneumoniae* to human lung A549 cells. A549 lung cells were pretreated with 2 mM NAC and exposed to CuONPs for 24 h. This was followed by incubation with *S. pneumoniae* serotype 4 at an MOI of 10 for 2 h. Afterwards, the cells were washed, trypsinized for 5 minutes, and lysed with saponin. Serial dilutions were made and 100 μL of each were streaked onto soy tryptic 5% sheep blood agar plates and cultured overnight at 37ºC in a humidified 5% CO_2 atmosphere. Colony forming units (CFU) were counted, and CFU/mL was determined. Results are the mean and SEM of five independent experiments performed in duplicate. * $P < 0.05$ using a student's *t*-test assuming unequal variances.

However, when NAC was added in the absence of CuONPs we did not see a significant change in pneumococcal adhesion. This suggests that NAC itself does not affect adhesion and that any adhesion could be solely attributed to CuONP-mediated effects. When NAC was added in conjunction with CuONPs there was decreased pneumococcal adhesion as compared to only CuONP exposure. Although the decrease in pneumococcal adhesion after NAC treatment was not significant, it shows a trend towards control levels. Taken together, *S. pneumoniae* adhesion was increased in CuONP treated A549 cells and this is thought to be the result of increased cell death. NAC-amelioration of cell death is thought to be the reason for the decreased adhesion capability of *S. pneumoniae* after CuONP exposure.

NAC is only one compound with potential of reversing the toxic effects of CuONPs. Since NAC serves to inhibit the early stages of cell death by limiting the production of toxic ROS species, it is considered a "gold standard" for these experiments. Inhibiting an early step of cell death is easier than attempting to inhibit a later step where a cell may be already committed to its demise. Apoptotic and necrotic inhibitors were thought to be potential agents for ameliorating CuONP toxicity. Cell viability was measured after pre-treatment with Z-VAD fmk or necrostatin-1 followed by increasing concentrations of CuONPs **(Fig 3.1.15).** Both Z-VAD-fmk **(Fig 3.1.15A)** and necrostatin-1 **(Fig 3.1.15B)** were tolerated well in the absence of CuONPs as evidenced by viabilities around 100%. This was considered desirable because both compounds were dissolved in DMSO, which is known to have toxic effects. Z-VAD-fmk was unable to restore cell viability in any of the CuONP concentrations used. This was not surprising because apoptosis was not thought to be a major cell death pathway. However, necrostatin-1 lead to further decreases in cell viability in addition to the decreases observed with just CuONP

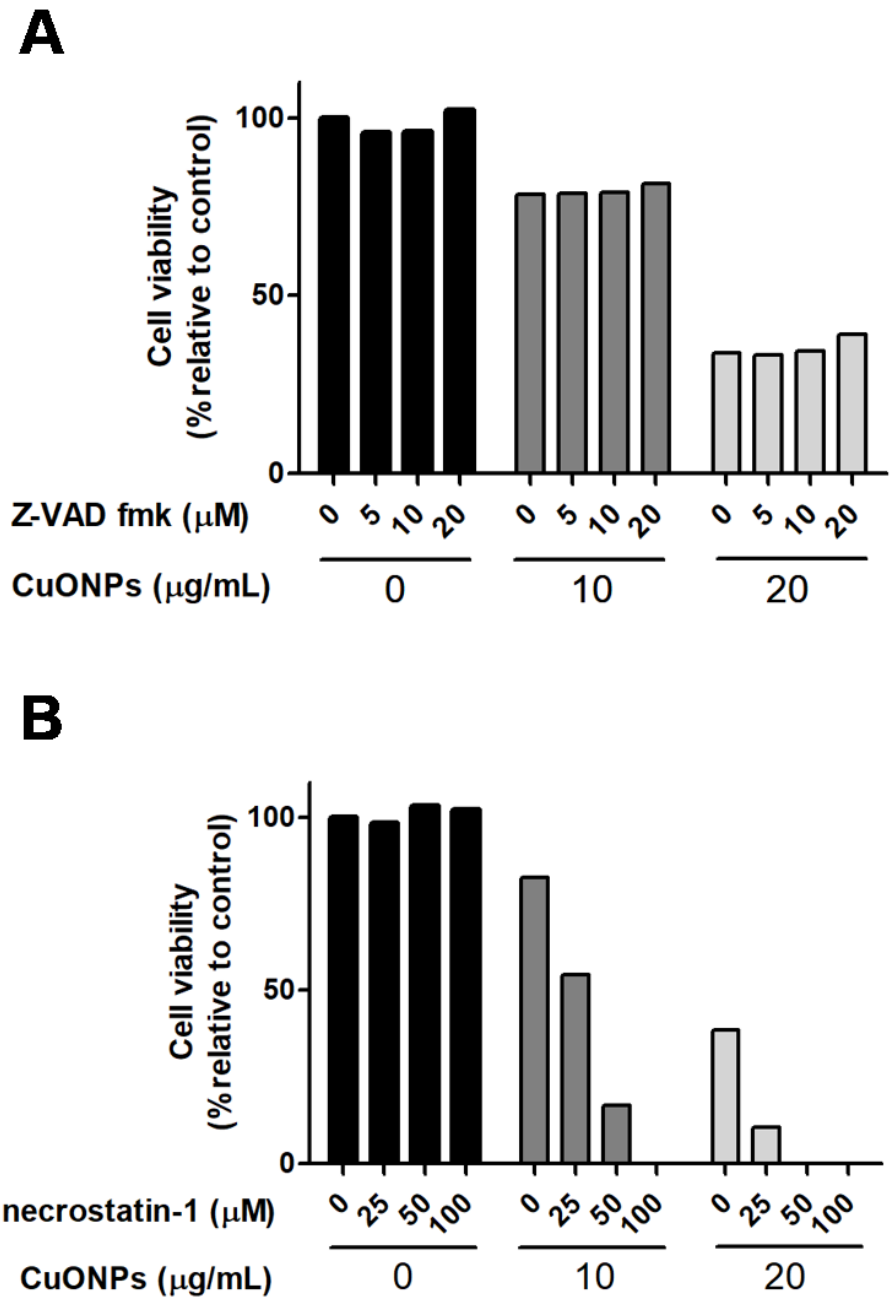

Figure 3.1.15. Z-VAD fmk and necrostatin-1 fail to restore cell viability after CuONP exposure. A549 cells were pretreated with increasing concentrations of Z-VAD fmk (**A)** or necrostatin-1 **(B)** prior to exposure CuONPs for 24 h. Cell viability was measured using an alamarBlue Proliferation assay as previously described **(A and B).** Results are the mean of one experiment done in duplicate.

exposure. This synergistic toxicity was shown to be dependent on necrostatin-1 concentration, with 100 μM being able to result in 0% cell viability in conjunction with the smallest CuONP dose (10 μg/mL). This was surprising because necrostatin-1 was well tolerated by itself, and CuONP toxicity was hypothesized to occur through necrotic mechanisms.

Finding inhibitors that can ameliorate toxicity can be similar to a "fishing expedition." Sometimes it is not known what drugs will work, but classifying agents on whether they reverse cytotoxicity can certainly provide key mechanistic insights into the pathways involved in toxicity. Two more compounds were investigated for their potential to reverse CuONP toxicity. First, cyclosporine A (CsA) was used because it blocks mitochondrial permeability during necrosis **[147]**. Second, wortmannin was used because autophagy has been linked to CuONP-mediated cell death **[148]**. Cell death was measured after pre-treatment with cyclosporine A or wortmannin followed by increasing concentrations of CuONPs **(Fig 3.1.16)**. In CuONP-exposed A549 cells without CsA, cell viability was 50%, which was further decreased to 25% in the presence of cyclosporine A **(Fig 3.1.16A)**. These results were similar to the necrostatin-1 experiments where there was increased potency of CuONPs after inhibitor pre-treatment. On the other hand, wortmannin pre-treatment lead to a modest restoration of cell viability after CuONP exposure **(Fig 3.1.16B)**. It is important to note that wortmannin itself is slightly toxic, reducing cell viability by about 15% in the absence of CuONPs. Wortmannin was able to rescue A549 cells from CuONP-induced cell death, however the rescue was modest, at about 20%.

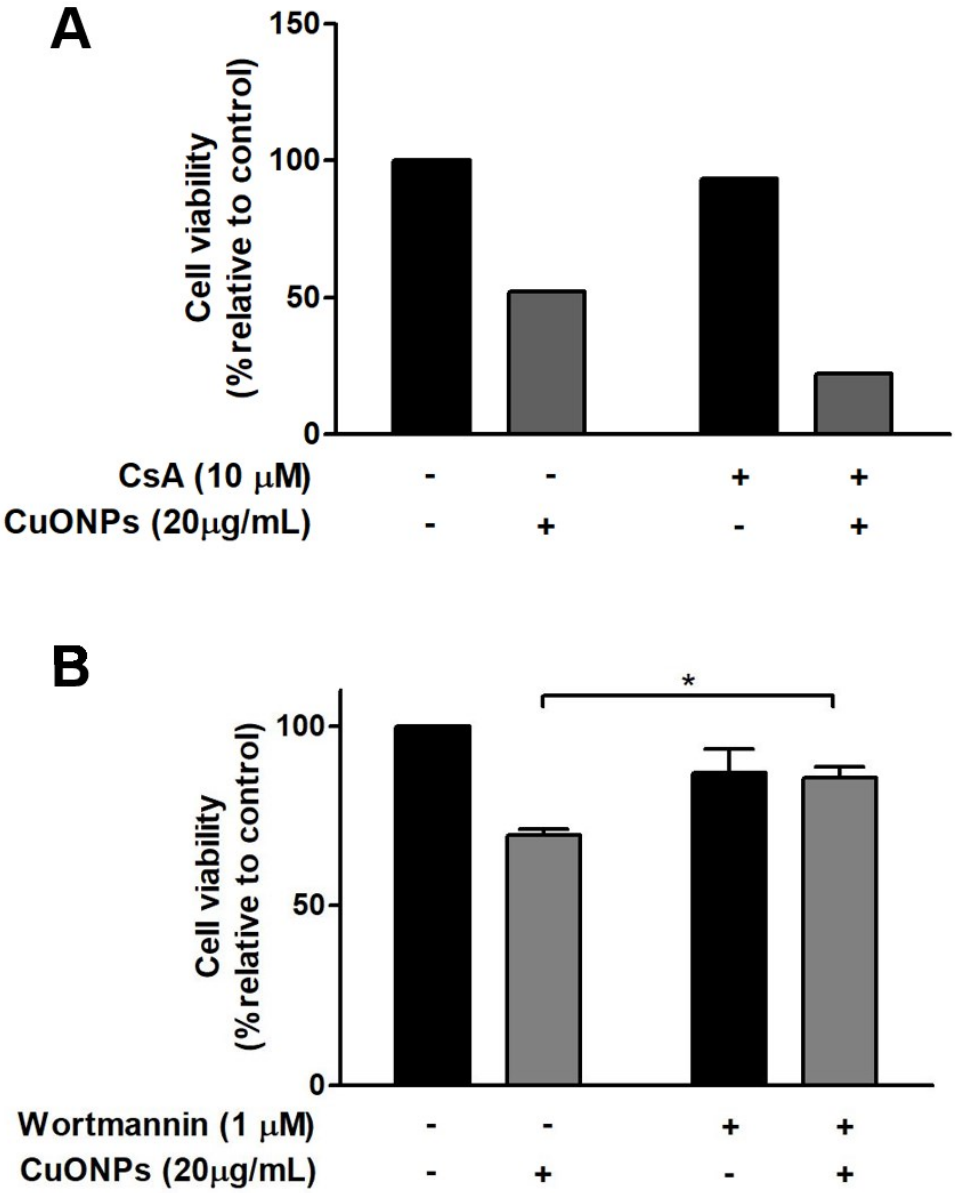

Figure 3.1.16. Wortmannin, but not cyclosporin restores cell viability after CuONP exposure. A549 cells were pretreated with CsA (**A)** or Wortmannin **(B)** prior to CuONP exposure for 24 h. Cell viability was measured using an alamarBlue Proliferation assay as previously described **(A and B).** Results are the mean and SEM of one (**A)** or two **(B)** independent experiments done in duplicate. * $P < 0.05$ using a student's *t*-test assuming unequal variances.

3.4 Exposure of CuONPs at an air-liquid interface

Submerged cell culture systems remain a gold standard in toxicology testing as a result of their cost-effectiveness and ability to screen a wide-range of toxicological doses not available to more robust animal models. Although results are beneficial and provides key mechanistic insights, this may not be a representative of true NP inhalation exposures where lung cells are exposed to air, and not liquid. To overcome this limitation, a novel exposure system was utilized as described in Section 2.3.2. Instead of a liquid-based delivery system, CuONPs were delivered using a spark discharge system between two metal electrodes and delivered to A549 cells within an InvitroCell exposure system **(Fig 3.2.1)** . N_2, O_2 and CO_2 were mixed proportionally to mimic ambient air, and the flow was controlled at 10 mL/min to properly mimic the flow that alveoli would be typically exposed to. Flow control is important to prevent the air itself from dislodging A549 cells, and to promote proper NP-sedimentation characteristics as opposed to impaction.

The dose delivered to submerged cultured cells can only be ascertained during initial treatment, but agglomeration and aggregation can lead to uncertainties in cellular dose. On the other hand, NPs delivered via ALI can be constantly monitored for size (nm), and number (particles/cm^3) using the SMPS. Whereas submerged NPs were about 30 nm in size, CuONPs delivered via ALI were approximately 5 nm as measured by SMPS (**Fig. 3.2.2A).** In addition, these particles were more normally distributed than NPs used in submerged studies, exhibiting a much lower geometric standard deviation (more monodispersed) and minimal skewness and kurtosis. In contrast to the nano-rods from submerged studies, NPs from ALI studies exhibited a more spherical morphology **(Fig 3.2.2B)**.

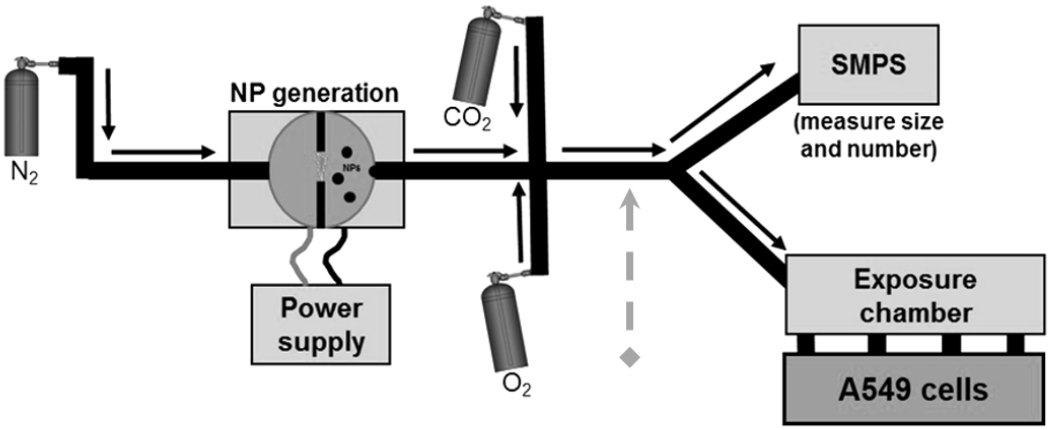

Figure 3.2.1. **Simplified schematic of NP generation and delivery at an ALI.** Constant voltage was applied to the generation chamber and CuONPs were generated by a spark discharge between two copper electrodes. Nitrogen (N_2) carried the NPs from the generation chamber and was supplemented with oxygen (O_2) and carbon dioxide (CO_2). From here, NPs were either taken to the size mobility particle sizer (SMPS) for characterization (size and distribution), or carried to the exposure chamber where NPs were delivered to A549 cells cultured on trans-well inserts. The dashed arrow denotes where the HEPA-filter was added to remove NPs for an air exposure control. Black arrows denote the direction of airflow.

It is important to note however that NPs collected for TEM analysis were collected at a charged anode via electrostatic precipitation using an aerosol sampler. As a result, TEM of ALI NPs may not be truly representative of the total NP population.

Despite a different size, morphology and delivery system, NPs generated by an ALI were investigated for their ability to increase bacterial adhesion. It was hypothesized that adhesion would be increased because NPs delivered at an ALI result in increased cell death at 4 h. Since cell death is thought to be directly involved in adhesion, the hypothesis was extended to include any NP exposure system capable of leading to cell death. Indeed, when A549 cells were exposed to CuONPs delivered by an ALI for 4 h, there was increased adhesion of *S. pneumoniae* (**Fig 3.2.3).** To rule out any effects of the ALI system not directly attributable to NPs (eg: ozone generation, air flow), an air-control was used which is the same exposure procedure, but NPs are filtered out immediately prior to delivery. It was shown that air-exposed A549 cells had no change in *S. pneumoniae* adhesion as compared to control. As a result, it was concluded that CuONPs are the responsible agent of increased pneumococcal adhesion, likely attributable to the increased cell death caused by the CuONPs.

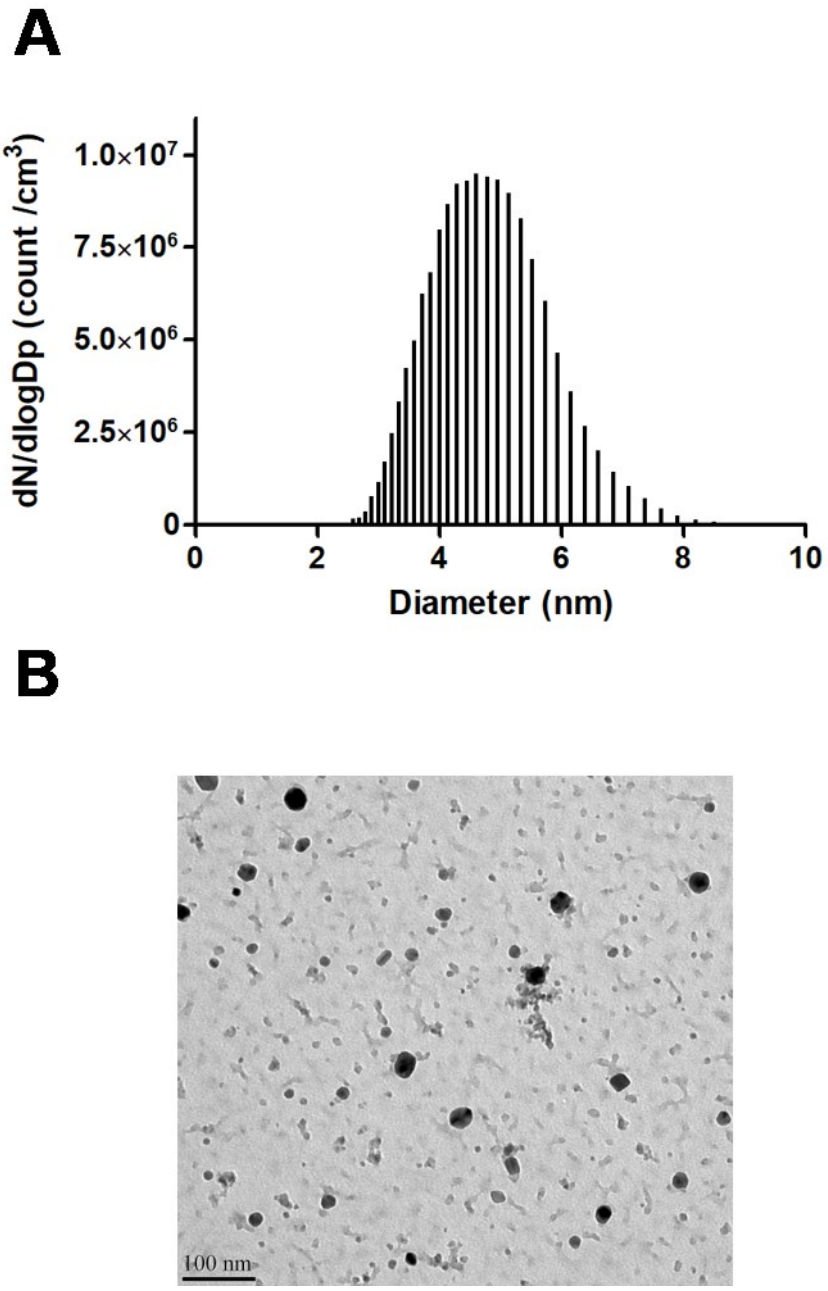

Figure 3.2.2. CuONPs generated for ALI are spherical and approximately 5 nm in diameter. Monodispersed CuONPs were generated as previously described, and size distribution and number was analyzed every 5 minutes using a size mobility particle sizer (SMPS) **(A)**. CuONPs were generated and collected onto nickel-plated grids for 24 h by electrostatic precipitation using a Nanometer Aerosol Sampler and analyzed using TEM **(B)**.

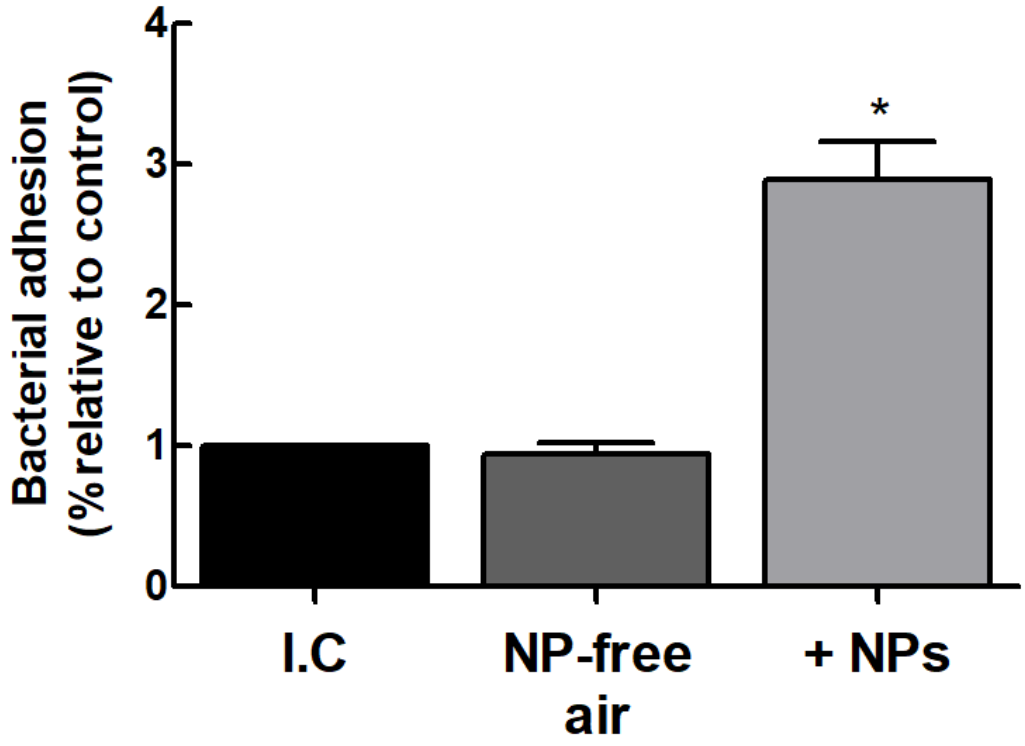

Figure 3.2.3. Adhesion of *S. pneumoniae* to human lung A549 cells is enhanced following exposure to CuONPs at an air-liquid interface. A549 lung cells were exposed to CuONPs for 4 h at an air-liquid interface as previously described. This was followed by incubation with *S. pneumoniae* serotype 4 at an MOI of 10 for 2 h. Afterwards, the cells were washed, trypsinized for 5 minutes and with saponin. Serial dilutions were made and 100 µL of each were streaked onto soy tryptic 5% sheep blood agar plates and cultured overnight at 37 ºC in a humidified 5% CO_2 atmosphere. Colony forming units (CFU) were counted, and CFU/mL was determined. Results are the mean and SEM of two independent experiment(s). * $P < 0.05$ using a student's *t*-test assuming unequal variances. I.C: Incubator control.

CHAPTER 4: DISCUSSION

4.1 NP toxicology is important for public health

The utilization of NPs in an ever-growing technology industry, coupled with increased combustion of fossil fuels, and increased occupational exposure has made NPs an important focus in research. Overall, toxicology is important for Public Health, as basic science research helps to inform future epidemiological studies, and vice-versa. Together, epidemiology and toxicology help inform health risk assessments for which policies and guidelines can be generated and enacted. Indeed, establishing a biological gradient (dose response relationship) and biological plausibility (support of an association) will help further the case that metal NPs, such as copper, are toxic. In the case of welders, occupational health measures can be undertaken to limit exposures to NPs generated through welding processes.

4.2 CuONPs are toxic to A549 cells and increase S. pneumoniae adhesion

Epidemiological studies are limited in their ability to study toxicological exposures. Indeed, it can be difficult to quantify exposures, and there are many covariates attributable to an association. For example, many welders also smoke cigarettes, which has been strongly linked to respiratory diseases, such as pneumonia **[149]**. As a result, *in vitro* studies provide a suitable surrogate to establish potential dose-response data. Exposure to welding fumes collected on a filter paper to A549 cells did increase pneumococcal adhesion, but the heterogeneity of metal fumes makes assigning toxicity to any one particular metal difficult **[44]**. It is likely that many metals are capable of leading to increased adhesion since many metals elicit similar inflammation and oxidative stress responses. For example, copper and iron both participate in Fenton reactions to generate

hydrogen peroxide to promote oxidative damage **[91,92]**. Although copper generally makes up a small proportion of welding fumes, copper NPs were chosen as the primary metal because it has a strong causal relationship between exposure and increased adhesion of *Klebsiella pneumoniae* **[142]**. Taken together, the work presented here can be applied to other metals of interest. Since welding fumes are often enriched in iron, this metal was also investigated for its cytotoxic potential.

For submerged culture systems, I made CuONPs using copper sulfate and NaOH to promote nucleation of the NPs. This method is quite beneficial because it can be easily scaled up for larger yields, and longer reactions increase the nucleation time resulting in larger particles. Many studies use other additives such as ascorbic acid for stability, or as capping agents, such as citrate **[150,151]**. I decided against adding any extra components during synthesis as these highly manipulated particles may no longer be representative of welding fumes. In other words, I wanted a pure, naked NP. However, one downside is that these nucleation reactions become more unpredictable in terms of size and shape. Future experiments could make CuONPs with added stabilizers and capping agents and their toxicity then compared to naked CuONP to observe any differences.

Technically, as long as our synthesized CuONPs were less than 100 nm in diameter along one dimension, they could be considered a 'nanoparticle'. In this case however, size matters, and a smaller particle was desired over a larger one. This is because a smaller particle can penetrate more deeply into alveolar regions **[137]**. Welding fumes are also enriched in nanoscale particles, with size varying based on welding technique, and type of metal used **[45]**. Although nanoparticles contribute little to fume mass, they contribute significantly to the total number of particles. Moreover, many studies investigating CuONP

toxicity use NPs with a size range anywhere between 1 nm and 50 nm. As a result, I would be content with a NP less than 50 nm so my results could be more easily compared to other toxicology studies. SMPS data showed that these particles were approximately 30 nm, which was a desired outcome **(Fig 3.1.1).** However, TEM showed that these particles were not spherical, possibly a result of not using capping or stabilizer agents during CuONP synthesis **(Fig 3.1.2)**. Welding fume particles are heterogenous in nature, with different metal composition, size and shape. Other studies have shown CuONPs as rods, or other unique shapes **[152]**. As a result, there is likely no true representative NP found in welding fumes so extrapolating toxicity data from only one type of NP should be done carefully.

XPS data **(Fig 3.1.3)** and XRD data **(Fig 3.1.4)** were also done to analyze these CuONPs further. Surprisingly, my CuONPs lined up perfectly with CuONPs generated elsewhere **[145,146].** This was a positive finding since it lent credibility to the idea that my CuONP particles may not be completely unique and may be somewhat representative of copper NPs found in welding fumes. It was found that my CuONPs had a high surface area providing more sites for reaction than a more spherical shape would. It was then concluded that these particles were likely to be acutely toxic based on the shape due to the high reactivity.

Additional characterization methods should also be performed to better determine whether these CuONPs are truly representative of particles of welding fumes. For example, charge distribution and deviation from the classic Boltzmann Distribution could be measured. Additionally, the zeta potential could be measured to determine electrokinetic potential of CuONPs in suspension.

Dissolution of CuONPs into toxic Cu ions is probably the biggest factor in driving toxicity. If there was no dissolution, there would be little toxicity. Interestingly, it was found that dissolution of CuONPs did not require the presence of cells **(Fig 3.1.5)**. This is in contrast of AgNPs, which require the acidic conditions of the lysosome for dissolution **[101]**. As a result, AgNPs function as a Trojan Horse, only resulting in dissolution once intracellular. Essentially, this leads to killing from within, versus CuONP having potential to attack extracellularly. Moreover, there was rapid dissolution of CuONPs into copper ions. This is important because toxicity would occur rapidly, preventing any sufficient adaptive response from the target cells such as sequestration **[153]**. It is still possible that CuONPs can still be taken up by cells, and after cell death has occurred Cu ions are rapidly released back into the media. This might create a situation where a NP/ion is only in the cell for a brief time, so accurately capturing intracellular copper may be difficult. Sublethal doses that prevent cell lysis, or compounds that could bind to intracellular copper preventing subsequent release may allow for better determination.

Differences in dissolution kinetics is extremely important to consider. If dissolution is slower in one solution versus than another than you will see differences in toxic responses. Cells and tissues are all exposed to different milieu, and as a result would likely have different toxic responses to the same NP. RPMI is great for cell culture, but may not truly represent the lung cell environment. ALF and Gamble's solution were used to represent intracellular lysosomes, and extracellular milieu, respectively **[154-156]**. Importantly, both solutions have different pHs. Whereas AgNPs required low pH for dissolution, CuONPs had dissolution in both ALF (pH =4.5) and Gamble's solution (pH 7.4). This is in slight disagreement with other papers which showed a more pronounced pH

effect on dissolution rate of CuONPs **[157-159]**. ALF and Gamble's solution have many components in common, such as NaCl, sodium citrate, and sulfate, so it is likely that one of these components is facilitating dissolution. The fact that PBS had a lower dissolution rate than water suggests that phosphate may inhibit CuONP dissolution. Since dissolution was rapid in our lung fluid solutions (ALF and Gamble's), it is likely that results would be representative of NPs in inhaled welding fumes.

CuONP-treated cells grew more slowly, and had considerable rounding, and detachment from culture dishes as visualized by light microscopy. This suggested that there was significant toxicity associated with CuONPs. This was expected because dissolution was rapid providing a large acute bolus of toxic Cu ions to the cells. I used an alamarBlue assay to confirm this, and found that there was considerable decrease in the reduction of dye, implying a defect in cellular metabolism **(Fig 3.1.7)**. These results are in agreement with other studies that show that CuONPs are toxic to a wide range of mammalian cell types. Not surprisingly, there was also a decrease in cell viability the longer a cell was exposed to CuONPs. There appeared to be a lag in toxicity at 5 h, most likely a result of NPs not having been fully dissoluted.

An interesting experiment to do would be to incubate NPs in media without cells for 3 h to allow for complete dissolution. This would be followed by treating cells with that solution to see how toxicity would differ. This would provide more evidence that cells are not required for transformation of NPs, and that copper ions are the main culprit for toxicity. It would also remove any lag effects, with a faster and higher toxic response expected.

It has been suggested that cell death results from increased oxidative stress and inflammation. Indeed, there was increased intracellular ROS after 24 h CuONP exposure **(Fig 3.1.8)**. To measure ROS, cells were washed in PBS, and incubated in HBSS containing the DCFDA probe. This probe is cell-permeable, and once inside the cell and cleaved, becomes trapped. I propose that this assay is not adequate to measure oxidative stress for three reasons. First, washing the cells would remove any copper (which has been shown to be extracellular). Second, since copper is extracellular, many ROS species could be extracellular, and would be washed away. Third, cell lysis could release intracellular contents, which would again be washed away. To improve upon this, I decided to measure a more stable, extracellular product of ROS, lipid peroxidation, which has been previously shown to be increased after CuONP exposure **[160]**. CuONPs were hypothesized to increase peroxy-radical formation, which would lead to peroxidation of the C11-BODIPY probe, which is then incorporated into membranes. Measuring the excitation/emission shift allowed for a direct measuring of oxidative stress. It was found that lipid peroxidation had a larger fold increase than intracellular ROS as compared to control (no CuONP). This further suggested that oxidative damage may have an extracellular component. However, severely damaged cells have severely disrupted and fluid membranes which might affect how C11-BODIPY functions as a probe. Shorter time points, before complete cell death has occurred would provide a better lipid peroxidation result.

FeNPs were also investigated for their cytotoxic potential. FeNPs are a major component of welding fumes due to steel and other iron-containing metals **(Fig 3.1.9)**. Since the Fenton reaction provides a suitable mechanism by which to generate oxidants to damage cells, iron was hypothesized to be toxic. However, iron did not undergo

dissolution, suggesting that it remained as an NP. This was confirmed using light microscopy, which showed large aggregates that had precipitated, and that these NPs did not promote oxidative stress (ROS or lipid peroxidation). Some studies have shown that FeNP dissolution is much more dependent on pH, with higher dissolution occurring at low pH **[161]**. In the case of inhaled NPs, the lung milieu may not be acidic enough to promote dissolution of FeNPs into toxic Fe ions **[162]**. This raises the question as to whether FeNPs are endocytosed with dissolution in the lysosomes. It appears not in A549 cells since most aggregates appeared extracellularly, but ICP-MS of cell lysates would provide a more detailed conclusion. It is also possible that FeNPs require dissolution in macrophages which can be released to promote toxicity of A549 cells. Co-cultures may show that toxicity depends on the presence of multiple cells working together to promote toxicity.

Oxidative stress has been shown to promote inflammation in A549 cells. IL-6 and IL-8 have been shown to be secreted by A549 cells after exposure to respiratory syncytial virus **[163].** Perhaps more importantly, IL-6 has been shown to be important in the defense against *S. pneumoniae* in mice **[164]**. Although pneumococci can cause increased IL-6 production, it is possible that an inflammatory response could lead to attraction and extravasation of *S. pneumoniae* to sites of injury. Upregulation of NFkB transcription would result in increased production and secretion of IL-6, IL-8 and MCP-1 **[82]**. Multiplex ELISA showed slightly increased secretion of IL-6, IL-8 and MCP-1 **(Fig 3.1.10)**. These results were expected since there was considerable oxidative stress after CuONP treatment. MCP-1 was shown to not be increased as much as IL-6 and IL-8, which suggests that the pathways governing its synthesis and secretion may be largely independent. Other studies have shown that MCP-1 deficiency does not affect cytokine levels, nor has any effect on

murine survival after pneumococcal challenge **[165,166]**. Although the role of this inflammatory response with respect to *S. pneumoniae* migration is not well known, it could be investigated with a combination of specific knockdown of various cytokines/chemokines to elucidate the role of specific mediators. Pretreatment with anti-inflammatories to blunt inflammation or with LPS to promote inflammation prior to CuONP treatment could better show the importance of inflammation in pneumococcal adhesion.

In addition to inflammation, oxidative stress promotes cell death. It is important to note, that although inflammation and cell death are intimately linked, inflammation can occur without cell death, and vice versa. NPs have been shown to promote apoptosis at low doses, and necrosis at higher concentrations, but my CuONPs were shown to favor necrosis at most concentrations used **(Fig 3.1.11)**. This makes sense because my CuONPs had very rapid dissolution, so A549 cells were immediately met with a large bolus of toxic copper ions. It is possible that treatment with even lower concentrations of CuONPs could favor apoptosis, or even shorter time points, since it is possible that apoptotic pathways can occur. Necrosis is more an end-point than a pathway, so it is possible that regulated mechanisms are occurring early on, and as a result earlier time-points should be investigated. Nonetheless, necrosis is still a predominant outcome after CuONP exposure. Necrosis, and resultant necrotic lesions result in dysfunction to surrounding cellular structures to increase permeability **[167]**. As a result, it is possible that *S. pneumoniae* is not attracted to lesion sites as a result of inflammation, but more an ability to extravasate to damaged lesion sites, creating an opportunity for adhesion.

However, if it was simply a result of being present and having an opportunity to adhere, then adding *S. pneumoniae* directly to healthy A549 cells should still lead to increased adhesion. However, *S. pneumoniae* was found to not strongly adhere to healthy A549 cells, but exhibited remarkable adhesion after CuONP-exposure **(Fig 3.1.12)**. This suggests that there is something inherently different between healthy and CuONP-exposed A549 cells. Previous research shows that welding fume-exposed A549 cells had increased pneumococcal adhesion as a result of upregulation of the PAFR receptor **[20]**. This could be determined by measuring PAFR protein concentration, mRNA levels, or localization of the receptor to the plasma membrane. Since receptor interactions depends on *S. pneumoniae* capsule, and it was possible that the capsule itself could influence adhesion, different serotypes were used. All serotypes exhibited similar increased pneumococcal adhesion after CuONP exposure, suggesting that adhesion is not capsule-dependent. This is good, because prevalence of serotypes is always changing (based on surveillance and vaccination), so the ability for *S. pneumoniae* to adhere after CuONP exposure could change from year to year. Nonetheless, serotype 3 would be an interesting serotype to look at, because of it makes a lot of capsule, and through a different mechanism **[168]**. This would help to completely determine the exact role of capsule. Additionally a Δcps mutant that does not produce capsule could also be investigated with respect to adherence capability after CuONP exposure.

It is likely that the increased adhesion capability comes from changes from within A549 cells, and *S. pneumoniae* takes advantage of this to adhere. Direct effects of CuONPs on *S. pneumoniae* were not measured, since I have hypothesized that the pneumococci are not present during initial CuONP exposure, only arriving after cell death and Cu ions are

cleared. Nonetheless, it might be interesting to look at biofilm formation, and changes in other virulence factors of *S. pneumoniae* after CuONP exposure.

The ability to reverse the cell death and inflammation associated with CuONP exposure might provide support for the development of prophylactic treatments to prevent pneumonia in susceptible populations, such as welders. NAC was used because it is well tolerated, and is an excellent scavenger of oxidants. Since it inhibits ROS at an early stage of CuONP toxicity, it was thought that cell viability would be easily restored. Indeed, NAC was shown to restore viability caused by CuONP exposure, likely due to decreased oxidative stress. Although inflammation was not measured after NAC pretreatment and CuONP exposure, it would be wise to better investigate the causal role of inflammation in CuONP-induced cell death. Since NAC was present during CuONP exposure, it is possible that NAC interacted directly with the NP to prevent dissolution. Interestingly, NAC has been shown to interact with pro-death proteins such as Bax, so it possible that amelioration of cell death is somewhat independent of its antioxidant capacity **[169]**. As a result, the ability of NAC to decrease ROS and lipid peroxidation after CuONP exposure should be measured. Other antioxidants such as glutathione with a more direct antioxidant function, should be used to see whether a similar effect can be achieved. However, the challenge of exposing NAC at an ALI to lung cells would be problematic, but perhaps a nebulizer system could be used.

I have posited that the increased pneumococcal adhesion is a result of increased cell death. This led me to hypothesize that NAC, which results in increased cell viability, would lead to decreased pneumococcal adhesion after CuONP treatment. This furthered the idea that pneumococci adhere better to necrotic cells. Indeed, NAC led to a decrease toward

baseline in adhesion of pneumococci after CuONP exposure **(Fig 3.1.14)**. Since NAC has many functions inside the cell, it is difficult to conclude that preventing the cell death is solely responsible for the decreased adhesion. It is possible that cell death and adhesion are correlated, but are not part of the same causal pathway. Instead, inflammation and oxidative stress could induce cell death and increased pneumococcal adhesion by separate mechanisms.

Using downstream inhibitors allowed me to better determine the causal pathway linking CuONP exposure, inflammation and cell death to increased pneumococcal adhesion. For example, if inhibition of downstream cell death responses did not result in a change in pneumococcal adhesion then this would suggest that both mechanisms are independent. I also attempted to choose drugs with a broad range of downstream targets to have a better chance to block a response. I chose Z-VAD-fmk as it is a pan-caspase inhibitor, meaning that it inhibits most effector caspases during apoptosis. Necrostatin-1 was thought to be promising because CuONPs promote necrosis, and necrostatin-1 inhibits RIPK-1 involved in necrotic cell death. Cyclosporine A inhibits cell death by preventing mitochondrial permeabilization, which is implicated in both necrotic and apoptotic cell death. Lastly wortmannin inhibits autophagy by blocking formation of the autophagosome, and autophagy was shown to occur during CuONP-induced cell death [148] **(Fig 3.1.15 and Fig 3.1.16)**.

Some of the drugs worked as expected. First, Z-VAD-fmk did not rescue cells from death, which was expected because apoptosis was shown to not be predominant in CuONP-induced cell death. Necrostatin-1 and cyclosporine A both led to a synergistic effect with CuONP, leading to further decreases in cell viability after exposure. It may be possible that

inhibition of certain pathways pushed these cells into other pathways with more lethality. Lastly, wortmannin was shown to be moderately effective in restoring cell viability, although not to baseline levels since wortmannin itself is toxic. This would make pneumococcal adhesion assays more difficult since wortmannin is likely to have its own effects on adhesion. Other studies have shown that *S. pneumoniae* itself can induce autophagy in A549 cells, so autophagy induced by CuONPs could possibly sensitize A549 cells better to pneumococcal adhesion **[170]**. The role of autophagy in CuONP-induced pneumococcal adhesion could be an interesting research study. It would also help determine whether cell death and pneumococcal adhesion are in the same causal pathway, or simply correlated with one another.

4.3 CuONPs delivered at an ALI also increases S. pneumoniae adhesion

Submerged cell exposure systems are a popular method by which to study the toxicity of many different compounds, and as such remain a 'gold standard'. However, one limitation of submerged systems is that these conditions do not mimic lung conditions *in vivo*, where lung cells are exposed to air, not media. In a submerged exposure system, there could be agglomeration and aggregation of NPs, and interactions with compounds in the media that could result in NP property changes. ALI experiments utilize specialized inserts that are significantly more costly that plastic culture dishes. As a result, submerged culture exposures are useful as a rapid screening tool to find proper doses, and exposure times. After this has been validated, it becomes useful to then use ALI exposures as they are a better representation of actual exposures. Once ALI exposures have been validated, this would provide excellent evidence and rationale to obtain ethical approval to use *in vivo* animal models.

It is important to note that NPs in submerged and ALI exposure experiments are not the same. So it is important to draw conclusions independently, and compare the biological responses of each exposure. The biological responses obtained in each exposure system will help to better predict the types of NPs that are responsible for eliciting toxic responses.

The ALI exposure system was previously made and characterized by Kim *et al.* **[171]**. The generation of ozone and nitrogen oxides was previously measured by others in our lab and were taken into account when assigning toxicological profiles. The ability to simultaneously measure particle size and number during exposure means that a constant and verifiable dose can be achieved. Since these particles were not suspended in solution and aerosolized, there is no water correction to be applied.

TEM proved to be difficult to perform. TEM requires a sufficient amount of particles to be deposited onto grids to be viewed. As a result, the ALI system was run for 24 h and particles were collected at an anode using a nanometer aerosol sampler. Since only positively charged particles were collected, this may not be truly representative of total particles generated. Nonetheless, particles appeared to be roughly spherical as opposed to the rods synthesized for submerged systems.

Previous research by others at HERC has shown that CuONPs delivered at an ALI are toxic to A549 cells. However, this cell death is rather modest, with about 20-30% cell death after 4 h of exposure. This is opposed to submerged culture systems where I was getting ~50% with 20 μg/mL after 24 h. So it was wondered whether a different delivery method, different cell viability, and exposure time would lead to a similar increase in pneumococcal adhesion. Interestingly, CuONP delivery at an ALI led to a more robust

increase in pneumococcal adhesion as compared to submerged systems, despite a higher cell viability and shorter exposure time. As a result a submerged culture experiments may be underestimating the ability for CuONPs to promote *S. pneumoniae* adhesion to lung cells. Similar experiments using pre-treatment with NAC will help further determine the role of inflammation, oxidative stress, and cell death in increasing pneumococcal adhesion.

4.4 Conclusion

The results presented here suggest that CuONPs are toxic to A549 cells by promoting oxidative stress, leading to increased inflammation and cell death. This increased cell death is thought to lead to increased adherence of *S. pneumoniae* to lung cells. Welders are chronically exposed to metal NPs, such as copper, so this work provides evidence to develop policies to limit occupational exposures to metal NPs. This work is considered to be exploratory, and provides potential pathways, such as autophagy that further research can expand on. Overall, this work provides valuable information on the underlying pathogenic mechanisms that will ultimately aid in disease prevention strategies.

REFERENCES

1. Leu, H. S., Kaiser, D. L., Mori, M., Woolson, R. F. and Wenzel, R. P. (1989). **Hospital-acquired pneumonia. attributable mortality and morbidity.** *Am. J. Epidemiol.* **129***(6)*, 1258-1267

2. O'Brien, K. L., Wolfson, L. J., Watt, J. P., Henkle, E., Deloria-Knoll, M., McCall, N., Lee, E., Mulholland, K., Levine, O. S. and Cherian, T. (2009). **Burden of disease caused by *Streptococcus pneumoniae* in children younger than 5 years: Global estimates.** *The Lancet.* **374***(9693)*, 893-902

3. Bogaert, D., de Groot, R. and Hermans, P. (2004). ***Streptococcus pneumoniae* colonisation: The key to pneumococcal disease.** *The Lancet infectious diseases.* **4***(3)*, 144-154

4. Beachey, E. H. (1981). **Bacterial adherence: Adhesin-receptor interactions mediating the attachment of bacteria to mucosal surface.** *J. Infect. Dis.* **143***(3)*, 325-345

5. Bryce, J., Boschi-Pinto, C., Shibuya, K., Black, R. E. and WHO Child Health Epidemiology Reference Group. (2005). **WHO estimates of the causes of death in children.** *The Lancet.* **365***(9465)*, 1147-1152

6. Meehan, T. P., Fine, M. J., Krumholz, H. M., Scinto, J. D., Galusha, D. H., Mockalis, J. T., Weber, G. F., Petrillo, M. K., Houck, P. M. and Fine, J. M. (1997). **Quality of care, process, and outcomes in elderly patients with pneumonia.** *JAMA.* **278***(23)*, 2080-2084

7. Alfageme, I., Vazquez, R., Reyes, N., Munoz, J., Fernandez, A., Hernandez, M., Merino, M., Perez, J. and Lima, J. (2006). **Clinical efficacy of anti-pneumococcal vaccination in patients with COPD.** *Thorax.* **61***(3)*, 189-195

8. Koivula, I., Sten, M. and Makela, P. H. (1994). **Risk factors for pneumonia in the elderly.** *Am. J. Med.* **96***(4)*, 313-320

9. Jones, G., Steketee, R. W., Black, R. E., Bhutta, Z. A., Morris, S. S. and Bellagio Child Survival Study Group. (2003). **How many child deaths can we prevent this year?** *The lancet.* **362***(9377)*, 65-71

10. Gupta, D., Agarwal, R., Aggarwal, A. N., Singh, N., Mishra, N., Khilnani, G. C., Samaria, J. K., Gaur, S. N., Jindal, S. K. and Pneumonia Guidelines Working Group. (2012). **Guidelines for diagnosis and management of community- and hospital-acquired pneumonia in adults: Joint ICS/NCCP(I) recommendations.** *Lung India.* **29***(Suppl 2)*, S27-62

11. Schroeder, M. R. and Stephens, D. S. (2016). **Macrolide resistance in *Streptococcus pneumoniae*.** *Frontiers in cellular and infection microbiology.* **6**, 98

12. Patel, S. N., McGeer, A., Melano, R., Tyrrell, G. J., Green, K., Pillai, D. R., Low, D. E. and Canadian Bacterial Surveillance Network. (2011). **Susceptibility of *Streptococcus pneumoniae* to fluoroquinolones in Canada.** *Antimicrob. Agents Chemother.* **55***(8)*, 3703-3708

13. Cooper, M. A. and Shlaes, D. (2011). **Fix the antibiotics pipeline.** *Nature.* **472***(7341)*, 32-32

14. Wong, A., Marrie, T. J., Garg, S., Kellner, J. D., Tyrrell, G. J. and SPAT Group. (2010). **Welders are at increased risk for invasive pneumococcal disease.** *International Journal of Infectious Diseases.* **14***(9)*, e796-e799

15. Palmer, K. T., Poole, J., Ayres, J. G., Mann, J., Burge, P. S. and Coggon, D. (2003). **Exposure to metal fume and infectious pneumonia.** *Am. J. Epidemiol.* **157***(3)*, 227-233

16. Mitchell, A. and Mitchell, T. (2010). ***Streptococcus pneumoniae*: Virulence factors and variation.** *Clinical Microbiology and Infection.* **16***(5)*, 411-418

17. Hammerschmidt, S., Wolff, S., Hocke, A., Rosseau, S., Muller, E. and Rohde, M. (2005). **Illustration of pneumococcal polysaccharide capsule during adherence and invasion of epithelial cells.** *Infect. Immun.* **73***(8)*, 4653-4667

18. Feldman, C., Mitchell, T., Andrew, P., Boulnois, G., Read, R., Todd, H., Cole, P. and Wilson, R. (1990). **The effect of *Streptococcus pneumoniae* pneumolysin on human respiratory epithelium in vitro.** *Microb. Pathog.* **9***(4)*, 275-284

19. Brown, J. S., Gilliland, S. M. and Holden, D. W. (2001). **A *Streptococcus pneumoniae* pathogenicity island encoding an ABC transporter involved in iron uptake and virulence.** *Mol. Microbiol.* **40***(3)*, 572-585

20. Shirasaki, H., Nishikawa, M., Adcock, I. M., Mak, J. C., Sakamoto, T., Shimizu, T. and Barnes, P. J. (1994). **Expression of platelet-activating factor receptor mRNA in human and guinea pig lung.** *Am. J. Respir. Cell Mol. Biol.* **10***(5)*, 533-537

21. Shukla, S. D. (1992). **Platelet-activating factor receptor and signal transduction mechanisms.** *FASEB J.* **6***(6)*, 2296-2301

22. Snyder, F. (1985). **Chemical and biochemical aspects of platelet activating factor: A novel class of acetylated ether- linked choline- phospholipids.** *Med. Res. Rev.* **5***(1)*, 107-140

23. Cundell, D. R., Gerard, N. P., Gerard, C., Idanpaan-Heikkila, I. and Tuomanen, E. I. (1995). ***Streptococcus pneumoniae*** **anchor to activated human cells by the receptor for platelet-activating factor.** *Nature.* **377***(6548)*, 435-438

24. Shukla, S. D., Fairbairn, R. L., Gell, D. A., Latham, R. D., Sohal, S. S., Walters, E. H. and O'Toole, R. F. (2016). **An antagonist of the platelet-activating factor receptor inhibits adherence of both nontypeable *Haemophilus influenzae* and *Streptococcus pneumoniae* to cultured human bronchial epithelial cells exposed to cigarette smoke.** *International Journal of Chronic Obstructive Pulmonary Disease.* **11**, 1647

25. Kadioglu, A., Weiser, J. N., Paton, J. C. and Andrew, P. W. (2008). **The role of *Streptococcus pneumoniae* virulence factors in host respiratory colonization and disease.** *Nature Reviews Microbiology.* **6***(4)*, 288-301

26. AlonsoDeVelasco, E., Verheul, A. F., Verhoef, J. and Snippe, H. (1995). ***Streptococcus pneumoniae*****: Virulence factors, pathogenesis, and vaccines.** *Microbiol. Rev.* **59***(4)*, 591-603

27. Nelson, A. L., Roche, A. M., Gould, J. M., Chim, K., Ratner, A. J. and Weiser, J. N. (2007). **Capsule enhances pneumococcal colonization by limiting mucus-mediated clearance.** *Infect. Immun.* **75***(1)*, 83-90

28. Hyams, C., Camberlein, E., Cohen, J. M., Bax, K. and Brown, J. S. (2010). **The *Streptococcus pneumoniae* capsule inhibits complement activity and neutrophil phagocytosis by multiple mechanisms.** *Infect. Immun.* **78***(2)*, 704-715

29. Kostyukova, N. N., Volkova, M. O., Ivanova, V. V. and Kvetnaya, A. S. (1995). **A study of pathogenic factors of *Streptococcus pneumoniae* strains causing meningitis.** *FEMS Immunol. Med. Microbiol.* **10***(2)*, 133-137

30. Hammerschmidt, S., Wolff, S., Hocke, A., Rosseau, S., Muller, E. and Rohde, M. (2005). **Illustration of pneumococcal polysaccharide capsule during adherence and invasion of epithelial cells.** *Infect. Immun.* **73***(8)*, 4653-4667

31. Manso, A. S., Chai, M. H., Atack, J. M., Furi, L., Croix, M. D. S., Haigh, R., Trappetti, C., Ogunniyi, A. D., Shewell, L. K. and Boitano, M. (2014). **A random six-phase switch regulates pneumococcal virulence via global epigenetic changes.** *Nature communications.* **5**

32. Sanchez, C. J., Hinojosa, C. A., Shivshankar, P., Hyams, C., Camberlein, E., Brown, J. S. and Orihuela, C. J. (2011). **Changes in capsular serotype alter the surface exposure of pneumococcal adhesins and impact virulence.** *PLoS One.* **6***(10)*, e26587

33. Kim, J. O. and Weiser, J. N. (1998). **Association of intrastrain phase variation in quantity of capsular polysaccharide and teichoic acid with the virulence of *Streptococcus pneumoniae*.** *J. Infect. Dis.* **177***(2)*, 368-377

34. Simell, B., Auranen, K., Käyhty, H., Goldblatt, D., Dagan, R. and O'Brien, K. L. (2012). **The fundamental link between pneumococcal carriage and disease.** *Expert review of vaccines.* **11***(7)*, 841-855

35. Song, J., Dagan, R., Klugman, K. P. and Fritzell, B. (2013). **The relationship between pneumococcal serotypes and antibiotic resistance.** *Pediatr. Pol.* **88***(6)*, T25-T37

36. Brueggemann, A. B., Griffiths, D. T., Meats, E., Peto, T., Crook, D. W. and Spratt, B. G. (2003). **Clonal relationships between invasive and carriage streptococcus pneumoniae and serotype- and clone-specific differences in invasive disease potential.** *J. Infect. Dis.* **187***(9)*, 1424-1432

37. Weinberger, D. M., Malley, R. and Lipsitch, M. (2011). **Serotype replacement in disease after pneumococcal vaccination.** *The Lancet.* **378***(9807)*, 1962-1973

38. Kellner, J. (2011). **Update on the success of the pneumococcal conjugate vaccine.** *Paediatrics & child health.* **16***(4)*, 233-236

39. Gitelson, S. and Werczberger, A. (1964). **Welders' disease.** *Harefuah.* **67***(12)*, 444-445

40. Collen, M. (1947). **A study of pneumonia in shipyard workers, with special reference to welders.** *Journal of Industrial Hygiene and Toxicology.* **29***(2)*, 113-122

41. Buckup, H. (1966). **Occupational diseases of the bronchi and lungs due to inorganic dusts.** *Zentralbl. Arbeitsmed.* **16***(7)*, 203-210

42. Palmer, K. T. and Cosgrove, M. P. (2012). **Vaccinating welders against pneumonia.** *Occup. Med. (Lond).* **62***(5)*, 325-330

43. Almirall, J., Gonzalez, C. A., Balanzo, X. and Bolibar, I. (1999). **Proportion of community-acquired pneumonia cases attributable to tobacco smoking.** *CHEST Journal.* **116***(2)*, 375-379

44. Suri, R., Palmer, K., Ross, J., Coggon, D. and Grigg, J. (2012). **S104 exposure to welding fume and adhesion of *Streptococcus pneumoniae* to A549 alveolar cells.** *Thorax.* **67***(Suppl 2)*, A51-A51

45. Antonini, J. M., Taylor, M. D., Zimmer, A. T. and Roberts, J. R. (2004). **Pulmonary responses to welding fumes: Role of metal constituents.** *Journal of Toxicology and Environmental Health, Part A.* **67***(3)*, 233-249

46. Donaldson, K., Tran, L., Jimenez, L. A., Duffin, R., Newby, D. E., Mills, N., MacNee, W. and Stone, V. (2005). **Combustion-derived nanoparticles: A review of their toxicology following inhalation exposure.** *Part Fibre Toxicol.* **2**, 10

47. Ferin, J., Oberdörster, G. and Penney, D. (1992). **Pulmonary retention of ultrafine and fine particles in rats.** *American journal of respiratory cell and molecular biology.* **6***(5)*, 535-542

48. Sung, J. H., Ji, J. H., Yoon, J. U., Kim, D. S., Song, M. Y., Jeong, J., Han, B. S., Han, J. H., Chung, Y. H. and Kim, J. (2008). **Lung function changes in sprague-dawley rats after prolonged inhalation exposure to silver nanoparticles.** *Inhal. Toxicol.* **20***(6)*, 567-574

49. Zhang, H., Ji, Z., Xia, T., Meng, H., Low-Kam, C., Liu, R., Pokhrel, S., Lin, S., Wang, X. and Liao, Y. (2012). **Use of metal oxide nanoparticle band gap to develop a predictive paradigm for oxidative stress and acute pulmonary inflammation.** *ACS nano.* **6***(5)*, 4349-4368

50. Colvin, V. L. (2003). **The potential environmental impact of engineered nanomaterials.** *Nat. Biotechnol.* **21***(10)*, 1166-1170

51. Kessler, R. (2011). **Engineered nanoparticles in consumer products: Understanding a new ingredient.** *Environ. Health Perspect.* **119***(3)*, A120-A125

52. Salata, O. (2004). **Applications of nanoparticles in biology and medicine.** *J. Nanobiotechnology.* **2***(1)*, 3

53. Tiede, K., Boxall, A. B., Tear, S. P., Lewis, J., David, H. and Hassellöv, M. (2008). **Detection and characterization of engineered nanoparticles in food and the environment.** *Food Addit. Contam.* **25***(7)*, 795-821

54. Tan, M., Commens, C. A., Burnett, L. and Snitch, P. J. (1996). **A pilot study on the percutaneous absorption of microfine titanium dioxide from sunscreens.** *Australas. J. Dermatol.* **37***(4)*, 185-187

55. Food and Drug Administration. (2015) **FDA's approach to regulation of nanotechnology products**. **2015**

56. van de Goot, F., Krijnen, P. A., Begieneman, M. P., Ulrich, M. M., Middelkoop, E. and Niessen, H. W. (2009). **Acute inflammation is persistent locally in burn wounds: A pivotal role for complement and C-reactive protein.** *Journal of burn care & research.* **30***(2)*, 274-280

57. Heggers, J. P., Robson, M. C., Manavalen, K., Weingarten, M. D., Carethers, J. M., Boertman, J. A., Smith Jr, D. J. and Sachs, R. J. (1987). **Experimental and clinical observations on frostbite.** *Ann. Emerg. Med.* **16***(9)*, 1056-1062

58. Hersh, D., Weiss, J. and Zychlinsky, A. (1998). **How bacteria initiate inflammation: Aspects of the emerging story.** *Curr. Opin. Microbiol.* **1***(1)*, 43-48

59. Steele, R. H. and Wilhelm, D. L. (1966). **The inflammatory reaction in chemical injury. I. increased vascular permeability and erythema induced by various chemicals.** *Br. J. Exp. Pathol.* **47***(6)*, 612-623

60. Medzhitov, R. (2008). **Origin and physiological roles of inflammation.** *Nature.* **454***(7203)*, 428

61. Eming, S. A., Krieg, T. and Davidson, J. M. (2007). **Inflammation in wound repair: Molecular and cellular mechanisms.** *J. Invest. Dermatol.* **127***(3)*, 514-525

62. Corti, R., Hutter, R., Badimon, J. J. and Fuster, V. (2004). **Evolving concepts in the triad of atherosclerosis, inflammation and thrombosis.** *J. Thromb. Thrombolysis.* **17***(1)*, 35-44

63. Galli, S. J., Tsai, M. and Piliponsky, A. M. (2008). **The development of allergic inflammation.** *Nature.* **454***(7203)*, 445

64. Holgate, S. T., Church, M. K., Howarth, P. H., Morton, N., Frew, A. J. and Djukanović, R. (1995). **Genetic and environmental influences on airway inflammation in asthma.** *Int. Arch. Allergy Immunol.* **107***(1-3)*, 29-33

65. Chaudhari, N., Talwar, P., Parimisetty, A., Lefebvre d'Hellencourt, C. and Ravanan, P. (2014). **A molecular web: Endoplasmic reticulum stress, inflammation, and oxidative stress.** *Frontiers in cellular neuroscience.* **8**, 213

66. St-Pierre, J., Buckingham, J. A., Roebuck, S. J. and Brand, M. D. (2002). **Topology of superoxide production from different sites in the mitochondrial electron transport chain.** *J. Biol. Chem.* **277***(47)*, 44784-44790

67. Hassan, H. M. and Fridovich, I. (1979). **Intracellular production of superoxide radical and of hydrogen peroxide by redox active compounds.** *Arch. Biochem. Biophys.* **196***(2)*, 385-395

68. Bienert, G. P., Moller, A. L., Kristiansen, K. A., Schulz, A., Moller, I. M., Schjoerring, J. K. and Jahn, T. P. (2007). **Specific aquaporins facilitate the diffusion of hydrogen peroxide across membranes.** *J. Biol. Chem.* **282***(2)*, 1183-1192

69. Halliwell, B. and Chirico, S. (1993). **Lipid peroxidation: Its mechanism, measurement, and significance.** *Am. J. Clin. Nutr.* **57***(5 Suppl)*, 715S-724S; discussion 724S-725S

70. Buettner, G. R. (1993). **The pecking order of free radicals and antioxidants: Lipid peroxidation, α-tocopherol, and ascorbate.** *Arch. Biochem. Biophys.* **300***(2)*, 535-543

71. Wang, D., Kreutzer, D. A. and Essigmann, J. M. (1998). **Mutagenicity and repair of oxidative DNA damage: Insights from studies using defined lesions.** *Mutation Research/Fundamental and Molecular Mechanisms of Mutagenesis.* **400***(1)*, 99-115

72. Monk, L. S., Fagerstedt, K. V. and Crawford, R. M. (1989). **Oxygen toxicity and superoxide dismutase as an antioxidant in physiological stress.** *Physiol. Plantarum.* **76***(3)*, 456-459

73. Drevet, J. R. (2006). **The antioxidant glutathione peroxidase family and spermatozoa: A complex story.** *Mol. Cell. Endocrinol.* **250***(1-2)*, 70-79

74. Di Mascio, P., Murphy, M. E. and Sies, H. (1991). **Antioxidant defense systems: The role of carotenoids, tocopherols, and thiols.** *Am. J. Clin. Nutr.* **53***(1)*, 194S-200S

75. Meister, A. (1994). **Glutathione-ascorbic acid antioxidant system in animals.** *Journal of Biological Chemistry-Paper Edition.* **269***(13)*, 9397-9400

76. Mates, J. (2000). **Effects of antioxidant enzymes in the molecular control of reactive oxygen species toxicology.** *Toxicology.* **153***(1-3)*, 83-104

77. Barchowsky, A., Dudek, E. J., Treadwell, M. D. and Wetterhahn, K. E. (1996). **Arsenic induces oxidant stress and NF-kB activation in cultured aortic endothelial cells.** *Free Radical Biology and Medicine.* **21***(6)*, 783-790

78. O'Donnell, V. B., Spycher, S. and Azzi, A. (1995). **Involvement of oxidants and oxidant-generating enzyme(s) in tumour-necrosis-factor-alpha-mediated apoptosis: Role for lipoxygenase pathway but not mitochondrial respiratory chain.** *Biochem. J.* **310 (Pt 1)***(Pt 1)*, 133-141

79. Eom, H. and Choi, J. (2009). **Oxidative stress of CeO2 nanoparticles via p38-nrf-2 signaling pathway in human bronchial epithelial cell, beas-2B.** *Toxicol. Lett.* **187***(2)*, 77-83

80. Jaiswal, A. K. (2004). **Nrf2 signaling in coordinated activation of antioxidant gene expression.** *Free Radical Biology and Medicine.* **36***(10)*, 1199-1207

81. Lee, J. and Johnson, J. A. (2004). **An important role of Nrf2-ARE pathway in the cellular defense mechanism.** *BMB Reports.* **37***(2)*, 139-143

82. Tak, P. P. and Firestein, G. S. (2001). **NF-kappaB: A key role in inflammatory diseases.** *J. Clin. Invest.* **107***(1)*, 7-11

83. Aggarwal, B. B. (2003). **Signalling pathways of the TNF superfamily: A double-edged sword.** *Nature reviews immunology.* **3***(9)*, 745

84. Hansson, G. K. and Libby, P. (2006). **The immune response in atherosclerosis: A double-edged sword.** *Nature Reviews Immunology.* **6***(7)*, 508

85. Romero, F. J., Bosch-Morell, F., Romero, M. J., Jareno, E. J., Romero, B., Marin, N. and Roma, J. (1998). **Lipid peroxidation products and antioxidants in human disease.** *Environ. Health Perspect.* **106 Suppl 5**, 1229-1234

86. Ji, L. L. (1993). **Antioxidant enzyme response to exercise and aging.** *Med. Sci. Sports Exerc.* **25***(2)*, 225-231

87. Jomova, K., Vondrakova, D., Lawson, M. and Valko, M. (2010). **Metals, oxidative stress and neurodegenerative disorders.** *Mol. Cell. Biochem.* **345***(1-2)*, 91-104

88. Valko, M., Morris, H. and Cronin, M. (2005). **Metals, toxicity and oxidative stress.** *Curr. Med. Chem.* **12***(10)*, 1161-1208

89. Tsukihara, T., Aoyama, H., Yamashita, E., Tomizaki, T., Yamaguchi, H., Shinzawa-Itoh, K., Nakashima, R., Yaono, R. and Yoshikawa, S. (1995). **Structures of metal sites of oxidized bovine heart cytochrome c oxidase at 2.8 A.** *Science.* **269***(5227)*, 1069-1074

90. Marklund, S. L. (1982). **Human copper-containing superoxide dismutase of high molecular weight.** *Proc. Natl. Acad. Sci. U. S. A.* **79***(24)*, 7634-7638

91. Winterbourn, C. C. (1995). **Toxicity of iron and hydrogen peroxide: The fenton reaction.** *Toxicol. Lett.* **82**, 969-974

92. Pham, A. N., Xing, G., Miller, C. J. and Waite, T. D. (2013). **Fenton-like copper redox chemistry revisited: Hydrogen peroxide and superoxide mediation of copper-catalyzed oxidant production.** *Journal of catalysis.* **301**, 54-64

93. Ponka, P., Beaumont, C. and Richardson, D. R. (1998). **Function and regulation of transferrin and ferritin.** *Semin. Hematol.* **35***(1)*, 35-54

94. Goldstein, I. M., Kaplan, H. B., Edelson, H. S. and Weissmann, G. (1979). **Ceruloplasmin. A scavenger of superoxide anion radicals.** *J. Biol. Chem.* **254***(10)*, 4040-4045

95. Scheinberg, I. H. and Gitlin, D. (1952). **Deficiency of ceruloplasmin in patients with hepatolenticular degeneration (wilson's disease).** *Science.* **116***(3018)*, 484-485

96. Roberts, E. A. and Schilsky, M. L. (2008). **Diagnosis and treatment of wilson disease: An update.** *Hepatology.* **47***(6)*, 2089-2111

97. Pujalté, I., Passagne, I., Brouillaud, B., Tréguer, M., Durand, E., Ohayon-Courtès, C. and L'Azou, B. (2011). **Cytotoxicity and oxidative stress induced by different metallic nanoparticles on human kidney cells.** *Particle and Fibre Toxicology.* **8***(1)*, 10

98. Xia, T., Kovochich, M., Liong, M., Mädler, L., Gilbert, B., Shi, H., Yeh, J. I., Zink, J. I. and Nel, A. E. (2008). **Comparison of the mechanism of toxicity of zinc oxide and cerium oxide nanoparticles based on dissolution and oxidative stress properties.** *ACS nano.* **2***(10)*, 2121-2134

99. Li, Y., Bhalli, J. A., Ding, W., Yan, J., Pearce, M. G., Sadiq, R., Cunningham, C. K., Jones, M. Y., Monroe, W. A. and Howard, P. C. (2014). **Cytotoxicity and genotoxicity assessment of silver nanoparticles in mouse.** *Nanotoxicology.* **8***(sup1)*, 36-45

100. Ispas, C., Andreescu, D., Patel, A., Goia, D. V., Andreescu, S. and Wallace, K. N. (2009). **Toxicity and developmental defects of different sizes and shape nickel nanoparticles in zebrafish.** *Environ. Sci. Technol.* **43***(16)*, 6349-6356

101. Sweeney, S., Leo, B. F., Chen, S., Abraham-Thomas, N., Thorley, A. J., Gow, A., Schwander, S., Zhang, J. J., Shaffer, M. S. and Chung, K. F. (2016). **Pulmonary surfactant mitigates silver nanoparticle toxicity in human alveolar type-I-like epithelial cells.** *Colloids and Surfaces B: Biointerfaces.* **145**, 167-175

102. Alkilany, A. M. and Murphy, C. J. (2010). **Toxicity and cellular uptake of gold nanoparticles: What we have learned so far?** *Journal of nanoparticle research.* **12***(7)*, 2313-2333

103. Elzey, S. and Grassian, V. H. (2010). **Nanoparticle dissolution from the particle perspective: Insights from particle sizing measurements.** *Langmuir.* **26***(15)*, 12505-12508

104. Logue, S. and Martin, S. (2008). **Caspase activation cascades in apoptosis.** *Biochem. Soc. Trans.* **36**, 1-9

105. Chen, M. and Wang, J. (2002). **Initiator caspases in apoptosis signaling pathways.** *Apoptosis.* **7***(4)*, 313-319

106. Shiozaki, E. N., Chai, J. and Shi, Y. (2002). **Oligomerization and activation of caspase-9, induced by apaf-1 CARD.** *Proc. Natl. Acad. Sci. U. S. A.* **99***(7)*, 4197-4202

107. Bodmer, J., Holler, N., Reynard, S., Vinciguerra, P., Schneider, P., Juo, P., Blenis, J. and Tschopp, J. (2000). **TRAIL receptor-2 signals apoptosis through FADD and caspase-8.** *Nat. Cell Biol.* **2***(4)*, 241-243

108. Kagan, V. E., Tyurin, V. A., Jiang, J., Tyurina, Y. Y., Ritov, V. B., Amoscato, A. A., Osipov, A. N., Belikova, N. A., Kapralov, A. A. and Kini, V. (2005). **Cytochrome c acts as a cardiolipin oxygenase required for release of proapoptotic factors.** *Nature chemical biology.* **1***(4)*, 223-232

109. Voll, R. E., Herrmann, M., Roth, E. A., Stach, C., Kalden, J. R. and Girkontaite, I. (1997). **Immunosuppressive effects of apoptotic cells.** *Nature.* **390***(6658)*, 350

110. Taylor, R. C., Cullen, S. P. and Martin, S. J. (2008). **Apoptosis: Controlled demolition at the cellular level.** *Nature reviews Molecular cell biology.* **9***(3)*, 231

111. Fadok, V. A., Voelker, D. R., Campbell, P. A., Cohen, J. J., Bratton, D. L. and Henson, P. M. (1992). **Exposure of phosphatidylserine on the surface of apoptotic lymphocytes triggers specific recognition and removal by macrophages.** *J. Immunol.* **148***(7)*, 2207-2216

112. Ha, H. C. and Snyder, S. H. (1999). **Poly(ADP-ribose) polymerase is a mediator of necrotic cell death by ATP depletion.** *Proc. Natl. Acad. Sci. U. S. A.* **96***(24)*, 13978-13982

113. Trump, B. E., Berezesky, I. K., Chang, S. H. and Phelps, P. C. (1997). **The pathways of cell death: Oncosis, apoptosis, and necrosis.** *Toxicol. Pathol.* **25***(1)*, 82-88

114. Krysko, D. V., Berghe, T. V., D'Herde, K. and Vandenabeele, P. (2008). **Apoptosis and necrosis: Detection, discrimination and phagocytosis.** *Methods.* **44***(3)*, 205-221

115. Duprez, L., Takahashi, N., Van Hauwermeiren, F., Vandendriessche, B., Goossens, V., Berghe, T. V., Declercq, W., Libert, C., Cauwels, A. and Vandenabeele, P. (2011). **RIP kinase-dependent necrosis drives lethal systemic inflammatory response syndrome.** *Immunity.* **35***(6)*, 908-918

116. Calabrese, E. J. and Baldwin, L. A. (1997). **The dose determines the stimulation (and poison): Development of a chemical hormesis database.** *Int. J. Toxicol.* **16***(6)*, 545-559

117. Rainaldi, G., Ferrante, A., Indovina, P. L. and Santini, M. T. (2003). **Induction of apoptosis or necrosis by ionizing radiation is dose-dependent in MG-63 osteosarcoma multicellular spheroids.** *Anticancer Res.* **23***(3B)*, 2505-2518

118. Fiers, W., Beyaert, R., Declercq, W. and Vandenabeele, P. (1999). **More than one way to die: Apoptosis, necrosis and reactive oxygen damage.** *Oncogene.* **18***(54)*, 7719

119. Wang, X. (2001). **The expanding role of mitochondria in apoptosis.** *Genes Dev.* **15***(22)*, 2922-2933

120. Zhu, M., Wang, Y., Feng, W., Wang, B., Wang, M., Ouyang, H. and Chai, Z. (2010). **Oxidative stress and apoptosis induced by iron oxide nanoparticles in cultured human umbilical endothelial cells.** *Journal of nanoscience and nanotechnology.* **10***(12)*, 8584-8590

121. Ahamed, M., Akhtar, M. J., Siddiqui, M. A., Ahmad, J., Musarrat, J., Al-Khedhairy, A. A., AlSalhi, M. S. and Alrokayan, S. A. (2011). **Oxidative stress mediated apoptosis induced by nickel ferrite nanoparticles in cultured A549 cells.** *Toxicology.* **283***(2-3)*, 101-108

122. AshaRani, P., Low Kah Mun, G., Hande, M. P. and Valiyaveettil, S. (2008). **Cytotoxicity and genotoxicity of silver nanoparticles in human cells.** *ACS nano.* **3***(2)*, 279-290

123. Piao, M. J., Kang, K. A., Lee, I. K., Kim, H. S., Kim, S., Choi, J. Y., Choi, J. and Hyun, J. W. (2011). **Silver nanoparticles induce oxidative cell damage in human liver cells through inhibition of reduced glutathione and induction of mitochondria-involved apoptosis.** *Toxicol. Lett.* **201***(1)*, 92-100

124. Jeng, H. A. and Swanson, J. (2006). **Toxicity of metal oxide nanoparticles in mammalian cells.** *Journal of Environmental Science and Health Part A.* **41***(12)*, 2699-2711

125. Misra, S. K., Dybowska, A., Berhanu, D., Luoma, S. N. and Valsami-Jones, E. (2012). **The complexity of nanoparticle dissolution and its importance in nanotoxicological studies.** *Sci. Total Environ.* **438**, 225-232

126. Studer, A. M., Limbach, L. K., Van Duc, L., Krumeich, F., Athanassiou, E. K., Gerber, L. C., Moch, H. and Stark, W. J. (2010). **Nanoparticle cytotoxicity depends on intracellular solubility: Comparison of stabilized copper metal and degradable copper oxide nanoparticles.** *Toxicol. Lett.* **197***(3)*, 169-174

127. Palza, H. (2015). **Antimicrobial polymers with metal nanoparticles.** *International journal of molecular sciences.* **16***(1)*, 2099-2116

128. Chen, Z., Meng, H., Xing, G., Chen, C., Zhao, Y., Jia, G., Wang, T., Yuan, H., Ye, C. and Zhao, F. (2006). **Acute toxicological effects of copper nanoparticles in vivo.** *Toxicol. Lett.* **163***(2)*, 109-120

129. Badawy, A. M. E., Luxton, T. P., Silva, R. G., Scheckel, K. G., Suidan, M. T. and Tolaymat, T. M. (2010). **Impact of environmental conditions (pH, ionic strength, and electrolyte type) on the surface charge and aggregation of silver nanoparticles suspensions.** *Environ. Sci. Technol.* **44***(4)*, 1260-1266

130. Lynch, I. and Dawson, K. A. (2008). **Protein-nanoparticle interactions.** *Nano today.* **3***(1-2)*, 40-47

131. Harkema, J. R., Carey, S. A. and Wagner, J. G. (2006). **The nose revisited: A brief review of the comparative structure, function, and toxicologic pathology of the nasal epithelium.** *Toxicol. Pathol.* **34***(3)*, 252-269

132. Jones, N. (2001). **The nose and paranasal sinuses physiology and anatomy.** *Adv. Drug Deliv. Rev.* **51***(1-3)*, 5-19

133. Antunes, M. B. and Cohen, N. A. (2007). **Mucociliary clearance--a critical upper airway host defense mechanism and methods of assessment.** *Curr. Opin. Allergy Clin. Immunol.* **7***(1)*, 5-10

134. Fraser, I. P., Koziel, H. and Ezekowitz, R. A. B. (1998) **The serum mannose-binding protein and the macrophage mannose receptor are pattern recognition molecules that link innate and adaptive immunity**. **10**, 363-372

135. Zolnik, B. S., Gonzalez-Fernandez, A., Sadrieh, N. and Dobrovolskaia, M. A. (2010). **Minireview: Nanoparticles and the immune system.** *Endocrinology.* **151***(2)*, 458-465

136. Gehr, P., Green, F., Geiser, M., Hof, V. I., Lee, M. and Schürch, S. (1996). **Airway surfactant, a primary defense barrier: Mechanical and immunological aspects.** *Journal of aerosol medicine.* **9***(2)*, 163-181

137. Lippmann, M., Yeates, D. B. and Albert, R. E. (1980). **Deposition, retention, and clearance of inhaled particles.** *Br. J. Ind. Med.* **37***(4)*, 337-362

138. Lippmann, M. and Albert, R. E. (1968). **Use of monodisperse aerosols for studies on respiratory tract deposition and clearance.** *J. Air Pollut. Control Assoc.* **18***(10)*, 672-674

139. Hoet, P. H., Brüske-Hohlfeld, I. and Salata, O. V. (2004). **Nanoparticles–known and unknown health risks.** *Journal of nanobiotechnology.* **2***(1)*, 12

140. Ryman-Rasmussen, J. P., Tewksbury, E. W., Moss, O. R., Cesta, M. F., Wong, B. A. and Bonner, J. C. (2009). **Inhaled multiwalled carbon nanotubes potentiate airway fibrosis in murine allergic asthma.** *American journal of respiratory cell and molecular biology.* **40***(3)*, 349-358

141. Xia, T., Li, N. and Nel, A. E. (2009). **Potential health impact of nanoparticles.** *Annu. Rev. Public Health.* **30**, 137-150

142. Kim, J. S., Adamcakova-Dodd, A., O'Shaughnessy, P. T., Grassian, V. H. and Thorne, P. S. (2011). **Effects of copper nanoparticle exposure on host defense in a murine pulmonary infection model.** *Part Fibre Toxicol.* **8***(29)*, b32

143. Hatchard, T. and Dahn, J. (2004). **In situ XRD and electrochemical study of the reaction of lithium with amorphous silicon.** *J. Electrochem. Soc.* **151***(6)*, A838-A842

144. Bayindir, Z., Duchesne, P., Cook, S., MacDonald, M. and Zhang, P. (2009). **X-ray spectroscopy studies on the surface structural characteristics and electronic properties of platinum nanoparticles.** *J. Chem. Phys.* **131***(24)*, 244716

145. Ethiraj, A. S. and Kang, D. J. (2012). **Synthesis and characterization of CuO nanowires by a simple wet chemical method.** *Nanoscale research letters.* **7***(1)*, 70

146. Kumar, P. V., Shameem, U., Kollu, P., Kalyani, R. and Pammi, S. (2015). **Green synthesis of copper oxide nanoparticles using aloe vera leaf extract and its antibacterial activity against fish bacterial pathogens.** *BioNanoScience.* **5***(3)*, 135-139

147. Sharov, V. G., Todor, A. V., Imai, M. and Sabbah, H. N. (2005). **Inhibition of mitochondrial permeability transition pores by cyclosporine A improves cytochrome C oxidase function and increases rate of ATP synthesis in failing cardiomyocytes.** *Heart Fail. Rev.* **10***(4)*, 305-310

148. Sun, T., Yan, Y., Zhao, Y., Guo, F. and Jiang, C. (2012). **Copper oxide nanoparticles induce autophagic cell death in A549 cells.** *PLoS One.* **7***(8)*, e43442

149. Korczynski, R. (2000). **Occupational health concerns in the welding industry.** *Appl. Occup. Environ. Hyg.* **15***(12)*, 936-945

150. Xiong, J., Wang, Y., Xue, Q. and Wu, X. (2011). **Synthesis of highly stable dispersions of nanosized copper particles using L-ascorbic acid.** *Green Chem.* **13***(4)*, 900-904

151. Deng, D., Jin, Y., Cheng, Y., Qi, T. and Xiao, F. (2013). **Copper nanoparticles: Aqueous phase synthesis and conductive films fabrication at low sintering temperature.** *ACS applied materials & interfaces.* **5***(9)*, 3839-3846

152. Mott, D., Galkowski, J., Wang, L., Luo, J. and Zhong, C. (2007). **Synthesis of size-controlled and shaped copper nanoparticles.** *Langmuir.* **23***(10)*, 5740-5745

153. Dameron, C. T. and Harrison, M. D. (1998). **Mechanisms for protection against copper toxicity.** *Am. J. Clin. Nutr.* **67***(5 Suppl)*, 1091S-1097S

154. Herting, G., Wallinder, I. O. and Leygraf, C. (2007). **Metal release from various grades of stainless steel exposed to synthetic body fluids.** *Corros. Sci.* **49***(1)*, 103-111

155. Stebounova, L. V., Guio, E. and Grassian, V. H. (2011). **Silver nanoparticles in simulated biological media: A study of aggregation, sedimentation, and dissolution.** *Journal of Nanoparticle Research.* **13***(1)*, 233-244

156. Luoto, K., Holopainen, M., Karppinen, K., Perander, M. and Savolainen, K. (1994). **Dissolution of man-made vitreous fibers in rat alveolar macrophage culture and gamble's saline solution: Influence of different media and chemical composition of the fibers.** *Environ. Health Perspect.* **102 Suppl 5**, 103-107

157. Hsueh, Y., Tsai, P. and Lin, K. (2017). **pH-dependent antimicrobial properties of copper oxide nanoparticles in *Staphylococcus aureus*.** *International journal of molecular sciences.* **18***(4)*, 793

158. Anderson, A., McLean, J., McManus, P. and Britt, D. (2017). **Soil chemistry influences the phytotoxicity of metal oxide nanoparticles.** *International Journal of Nanotechnology.* **14***(1-6)*, 15-21

159. Shi, M., de Mesy Bentley, Karen L, Palui, G., Mattoussi, H., Elder, A. and Yang, H. (2017). **The roles of surface chemistry, dissolution rate, and delivered dose in the cytotoxicity of copper nanoparticles.** *Nanoscale.* **9***(14)*, 4739-4750

160. Sayes, C. M., Gobin, A. M., Ausman, K. D., Mendez, J., West, J. L. and Colvin, V. L. (2005). **Nano-C60 cytotoxicity is due to lipid peroxidation.** *Biomaterials.* **26***(36)*, 7587-7595

161. Baalousha, M. (2009). **Aggregation and disaggregation of iron oxide nanoparticles: Influence of particle concentration, pH and natural organic matter.** *Sci. Total Environ.* **407***(6)*, 2093-2101

162. Masuda, M., Sato, T., Sakamaki, K., Kudo, M., Kaneko, T. and Ishigatsubo, Y. (2015). **The effectiveness of sputum pH analysis in the prediction of response to therapy in patients with pulmonary tuberculosis.** *PeerJ.* **3**, e1448

163. Fiedler, M. A., Wernke-Dollries, K. and Stark, J. M. (1995). **Respiratory syncytial virus increases IL-8 gene expression and protein release in A549 cells.** *Am. J. Physiol.* **269***(6 Pt 1)*, L865-72

164. van der Poll, T., Keogh, C. V., Guirao, X., Buurman, W. A., Kopf, M. and Lowry, S. F. (1997). **Interleukin-6 gene-deficient mice show impaired defense against pneumococcal pneumonia.** *J. Infect. Dis.* **176***(2)*, 439-444

165. Gu, L., Tseng, S., Horner, R. M., Tam, C., Loda, M. and Rollins, B. J. (2000). **Control of T H 2 polarization by the chemokine monocyte chemoattractant protein-1.** *Nature.* **404***(6776)*, 407

166. Jones, M. R., Simms, B. T., Lupa, M. M., Kogan, M. S. and Mizgerd, J. P. (2005). **Lung NF-kappaB activation and neutrophil recruitment require IL-1 and TNF receptor signaling during pneumococcal pneumonia.** *J. Immunol.* **175***(11)*, 7530-7535

167. Jones, A. W. (1978). **Bleomycin lung damage: The pathology and nature of the lesion.** *Br. J. Dis. Chest.* **72***(4)*, 321-326

168. Watson, D. A. and Musher, D. M. (1990). **Interruption of capsule production in *Streptococcus pneumonia*e serotype 3 by insertion of transposon Tn916.** *Infect. Immun.* **58***(9)*, 3135-3138

169. Reid, A. J., Shawcross, S. G., Hamilton, A. E., Wiberg, M. and Terenghi, G. (2009). **N-acetylcysteine alters apoptotic gene expression in axotomised primary sensory afferent subpopulations.** *Neurosci. Res.* **65***(2)*, 148-155

170. Li, P., Shi, J., He, Q., Hu, Q., Wang, Y. Y., Zhang, L. J., Chan, W. T. and Chen, W. (2015). ***Streptococcus pneumoniae* induces autophagy through the inhibition of the PI3K-I/akt/mTOR pathway and ROS hypergeneration in A549 cells.** *PloS one.* **10***(3)*, e0122753

171. Kim, J. S., Peters, T. M., O'Shaughnessy, P. T., Adamcakova-Dodd, A. and Thorne, P. S. (2013). **Validation of an in vitro exposure system for toxicity assessment of air-delivered nanomaterials.** *Toxicology in Vitro.* **27***(1)*, 164-173